

UNIVERSIDADE FEDERAL DO RIO GRANDE DO SUL

INSTITUTO DE GEOCIÊNCIAS

PROGRAMA DE PÓS-GRADUAÇÃO EM GEOCIÊNCIAS

Elise Rachel Mulocher

Estudo das Argilas das Rochas Basálticas da Formação Serra Geral no Rio Grande do Sul.

**Argilominerais em lavas portadoras de ametista na
região do Alto Uruguai (RS), Província Magmática do
Paraná.**

ORIENTADOR – Prof. Dr. André Sampaio Mexias

BANCA EXAMINADORA

Prof. Dr. Milton Luiz Laquintinie Formoso– Instituto de Geociências,
Universidade federal do Rio Grande do Sul

Profa. Dra. Marcia Elisa Boscato Gomes – Instituto de Geociências,
Universidade federal do Rio Grande do Sul

Profa. Dra. Maria José Maluf de Mesquita - Instituto de Geociências,
Universidade Estadual de Campinas

Dissertação de Mestrado apresentada
como requisito parcial para a obtenção
do Título de Mestre em Geociências.

Resumo:

O derrame estudado é o sexto da sequência basáltica do Alto Uruguai, no norte do Rio Grande do Sul. Este derrame faz parte da Fm Serra Geral que é a parte brasileira do grande evento geológico: a formação da Província Magmática Paraná-Etendeka. Este derrame tem a seguinte estruturação interna: - nível basal contendo vesículas; nível intermediário com 10 a 25m de espessura, com fraturamento irregular e contendo no topo um nível macrovesicular interno, onde ocorrem os geodos (com diâmetros de milímetros a metros). Estes geodos são preenchidos principalmente por minerais de sílica como ametista, ágata e calcedônia, mas podem conter também calcita e zeolitas associadas; - nível superior, com 2 a 4m de espessura de basalto maciço; e – nível vesicular de topo, com 1 a 2 m de espessura, contendo vesículas (milimétricas a centimétricas) preenchidas por zeolitas, calcita, quartzo e argilominerais. Oito amostras destas rochas foram estudadas através de difratometria de raios X, petrografia, microscopia eletrônica e geoquímica de rocha total, com o objetivo de entender a gênese dos argilominerais presentes nestas rochas. A esmectita é o argilomineral presente em todas as rochas, principalmente ocupando a mesóstase. A celadonita ocorre somente no contato com os geodos e as vesículas. A esmectita é bem cristalizada, tem seu crescimento perpendicular às faces dos cristais primários e não ocorre nas zonas de alteração. As vesículas contêm diferentes gerações de argilominerais, com a esmectita sendo formada inicialmente, seguida da celadonita. A presença de esmectita como inclusão em apatita, seu aspecto de crescimento, associado à presença de celadonita somente nas zonas de maior alteração, sugerem que a esmectita pode ter a sua origem durante os processos tardi-magmáticos e a celadonita resulta de processos de alteração hidrotermal destas rochas.

Abstract:

The basalt flow deposit studied is the 6th of a basaltic sequence of the Alto Uruguai region in the Rio Grande do Sul state. This deposit is situated in the Serra Geral formation which is the Brazilian part of a big geological event: the formation of the Paraná-Etendeka magmatic province. This flow have the internal structures as: -a basal level that contains vesicles; - a medium level from 10 to 25m, irregularly fractured that contains at the top an internal macrovesicular level where we can find geodes (from few millimeters to few meters diameter). These geodes are principally filled with silica minerals as amethyst, agate and chalcedony, but can also have associated minerals as calcite and zeolites; - the superior level, from 2 to 4 m thick, of massive basalt; - and a vesicular level on the top, 1 to 2m thick, where vesicles (from millimeter to centimeter diameter) are filled with zeolites, calcite, quartz and clays. Eight rock samples were used for this study, by X-ray diffraction, petrography, electron microscopy and whole rock chemistry, with the aim to understand how the clays present in a basal flow could have formed. Smectite is the clay mineral that occurs in all samples, mainly in the mesostasis. Celadonite occurs only in the contact of the geodes and vesicles. Smectite is well crystallized, growing perpendicular to the phenocrystals surfaces and doesn't grow in the alteration zones. Vesicles contain different generations of clay minerals with a first one of smectite and a second of celadonite. The presence of smectites as inclusion in apatite, its growing aspects, along with the presence of celadonite only in the alteration zones suggest that smectites could be formed during the tardi-magmatic processes and celadonite represents the hydrothermal alteration product of this rock.

Sumário

Resumo:	ii
Abstract:.....	iii
I - Introdução.....	1
1. Mineralogia e Texturas do Derrame.....	2
2. Características Químicas do Derrame.....	3
3. A Distribuição das fases minerais tardias.....	5
II – Objetivos Gerais do Estudo.....	6

Texto completo submetido à Université de Poitiers e à Universidade Federal do Rio Grande do Sul

I. Introduction	10
II. Local geology.....	11
III. Material and methods.....	17
IV. Results.....	19
1. Macroscopic observations.....	19
2. Optical Microscope.....	20
General aspect of the basalt, reference sample BT.....	20
Evolution of the samples in function of the distance to the Geode.	21
3. XRD analys.	23
4. SEM on rock fragments Images.	25
5. SEM on slides EDS.	27
V. Discussions.	31
1. Macroscopic, fieldtrip interpretation.	31

2.	Optical Microscope.	31
3.	XRD analysis.	32
4.	SEM on rock fragments Images.	33
5.	SEM on slides EDS.	34
VI.	Conclusions.	35
	References.	37
	Appendix.	38

I - INTRODUÇÃO

A Bacia do Paraná é uma depressão intra cratônica com uma área de dimensões da ordem de 1,6 milhão de km², que foi preenchida por sedimentos marinhos e continentais do Devoniano ao Jurássico, acumulando uma espessura máxima de aproximadamente 7.000 metros em suas porções centrais. Ela contém, portanto, enormes volumes de sedimentos saturados em água e derrames e intrusões essencialmente basálticas. A combinação destes fatores, ao longo de uma história geológica que se estendeu por centenas de milhões de anos, criou as condições para a geração de fenômenos pós-magmáticos, de natureza hidrotermal, com possível influência na gênese de depósitos minerais de interesse econômico.

A região do Alto Uruguai, no norte do Rio Grande do Sul, apresenta uma sequência de derrames basálticos da Fm Serra Geral constituída por 12 derrames formando um pacote de aproximadamente 20.000 Km³ de rocha. O sexto derrame da sequência caracteriza-se por possuir estrutura do Tipo I (Gomes, 1996), apresentando na área estudada espessura entre 15m e 35m e a seguinte estratificação da base para o topo (Fig.1):

1. Nível vesicular basal - pouco espesso, em média de 50cm;
2. Nível central - é a porção mais espessa do derrame, pode ter entre 10 e 25m, dependendo da espessura total do derrame. Apresenta um padrão de fraturamento que não corresponde aos tipos “colunado” e “entablamento”, caracterizado por fraturas pouco pronunciadas, muito irregulares, que dão origem a grandes blocos com 1m a 2m de diâmetro. No topo deste nível, é comum a presença de um nível macrovesicular interno, formado por geodos de tamanhos variados (desde centimétricos, podendo atingir alguns metros de diâmetro), preenchidos principalmente por sílica, na forma de calcedônia, ágata e ametista, podendo ocorrer calcita e zeolitas (heulandita e mordenita) associadas;
3. Nível superior - esta zona situa-se acima do nível vesicular interno e é constituída por basalto maciço, não vesicular, intensamente fraturado, com fraturas preferencialmente horizontais, com espaçamento centimétrico. Este nível pode ter entre 2 e 4m de espessura. Nos derrames onde há mineralização, esta zona representa o nível estéril que marca o topo das galerias;

4. Nível vesicular de topo - com 1 a 2 m de espessura, contém vesículas milimétricas a centimétricas, preenchidas por zeolitas, calcita, quartzo e argilominerais, especialmente do tipo celadonita e Fe-saponita.

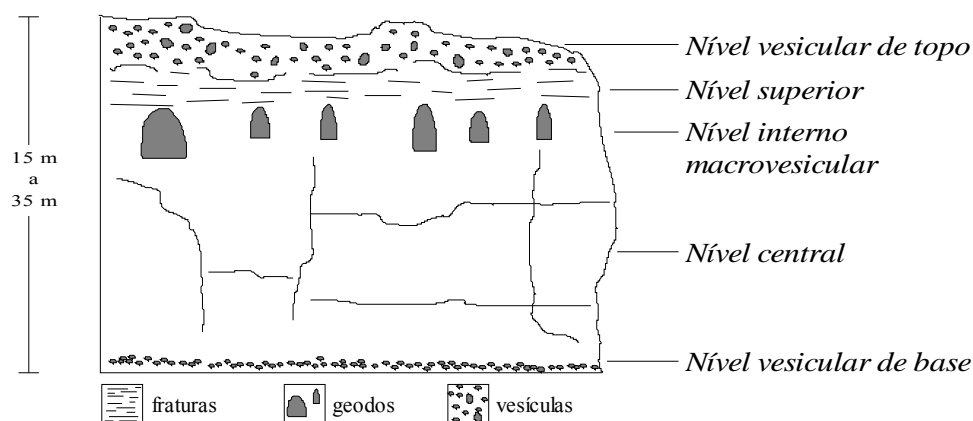


Fig. 1 Perfil esquemático de derrames do tipo I, mostrando suas diferentes estruturas internas (retirada de Gomes, 1996).

1. MINERALOGIA E TEXTURAS DO DERRAME

Estas rochas são constituídas por plagioclásio do tipo labradorita, augita, minerais opacos do tipo magnetita, titano-magnetita e ilmenita, olivina (que ocorre em todos os derrames deste grupo) e uma mesóstase de composição ácida nos interstícios dos grãos, onde aparecem também agulhas de apatita.

A granulação é fina, com cristais tabulares a ripiformes de plagioclásio, mais raramente são observados microfenocristais de piroxênio.

As texturas são predominantemente intersertais a intergranulares.

De modo geral, as texturas, mineralogia e morfologia dos grãos são constantes ao longo de toda a espessura do derrame. Variações texturais e mineralógicas somente são encontradas associadas à presença de geodos no nível vesicular interno onde a textura torna-se micro-porfírica, com microfenocristais de plagioclásio e augita imersos em uma matriz micro a criptocristalina com até 20% de mesóstase. Observa-se

também a presença, em grande quantidade, de minerais de alteração, especialmente argilominerais do tipo celadonita, que ocorrem principalmente nos espaços intersticiais e como produtos de alteração da olivina e, secundariamente, do piroxênio. É comum também a ocorrência de esmectita na mesóstase intersticial.

2. CARACTERÍSTICAS QUÍMICAS DO DERRAME

Os principais parâmetros químicos comumente utilizados e revisados por Peate (1989) para a caracterização dos diferentes tipos magmáticos da Fm Serra Geral são apresentados na tabela 1, juntamente com os valores correspondentes de cada derrame da região de Frederico Westphalen, dentre eles o derrame 6, e aplicados nos diagramas das figuras 2.11, 2.12, 2.13 e 2.14. Estes dados foram extraídos de Gomes 1996.

Tab 1- Parâmetros químicos e tipos magmáticos, definidos por Peate (1989), para as rochas vulcânicas básicas com teores intermediários e altos de TiO₂.

	est.	TiO ₂	P ₂ O ₅	SiO ₂	Fe ₂ O ₃	Sr	Ba
Urubici		3,3	0,45	50	14,2	600	450
Pitanga		2,9	0,35	47-52	14	400-600	340-700
Paranap		1,8-3,2	0,2-0,7	49-51,5	13,5	430	410
derrame 1	II	3,6-3,99	0,52	51,29-51,88	13,84-14,03	490-495	490-612
derrame 2	I	3,49-3,81	0,43-0,57	49,21-49,87	14,74-15,98	406-464	400-647
derrame 3	I	3,6-3,63	0,58-0,6	46,57-48,69	15,06-15,55	416-429	466-528
derrame 4	II	2,16-2,65	0,31-0,34	49,21-48,94	14,27-15,94	310-342	347-562
derrame 5	II	3,94	0,43	50,47	13,96	474	454
derrame 6	I	3,30-3,73	0,49-0,56	47,56-50,95	14,12-15,74	409-482	378-582
derrame 7	I	2,13-2,22	0,25	49,31-49,82	13,68-13,82	365-383	333-339
derrame 8	I	3,52-3,75	0,56-0,57	47,19-50,31	14,38-15,18	406-431	498-569
derrame 9	I	1,87-2,28	0,22-0,3	48,23-50,54	12,96-14,68	329-437	305-367
derrame 10	I	3,28	0,41	49	15,66	434	412
derrame 11	II	2,21-2,26	0,27-0,28	49,56-51,52	14,68-15,34	250-349	318-373

	est.	Zr	Sr/Y	Ba/Y	Zr/Y	Ti/Y	Ti/Zr
Urubici		270	10,5	11,5	7	500	60
Pitanga		200-440	10	9-14,5	5,5-8	350-700	50
Paranap		250	10,5	4,5-13	4,5-6	300-500	65
derrame 1	II	278	12,69-12,89	12,89-15,69	7,13-7,32	554-629	78-86
derrame 2	I	220-232	9,44-12,89	11,76-15,04	5,32-6,47	487-672	91-104
derrame 3	I	240-242	10,21-10,40	11,09-13,20	5,71-6,05	514-544	90
derrame 4	II	149-172	9,77-10	9,91-18,13	4,91-4,81	418-454	87-92
derrame 5	II	227	13,17	12,61	6,3	656	104
derrame 6	I	231-276	10,22-12,70	10,21-13,47	6,24-7,08	495-573	78-91
derrame 7	I	147	13,03-13,68	11,89-12,11	5,25	456-475	87-91
derrame 8	I	227-238	11,00-12,00	13-15	6	558-608	92-96
derrame 9	I	130-152	10,00-17,00	10,00-14,00	5	427-467	86-96
derrame 10	I	199	14	13,29	6,42	634	99
derrame 11	II	148-172	6,75-10,91	8,59-11,65	4,56-4,64	358-423	79-92

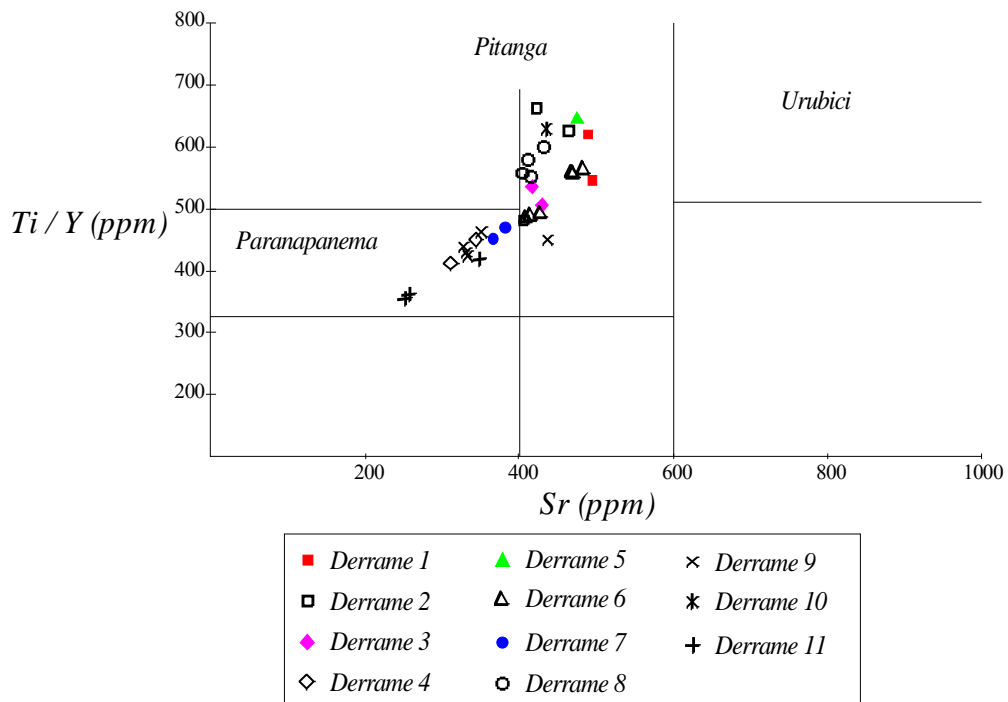


Fig. 2- Variações de Ti/Y e Sr nos derrames da região de Frederico Westphalen. O diagrama é subdividido (conforme Peate, 1989) nos campos que definem os diferentes tipos magmáticos.

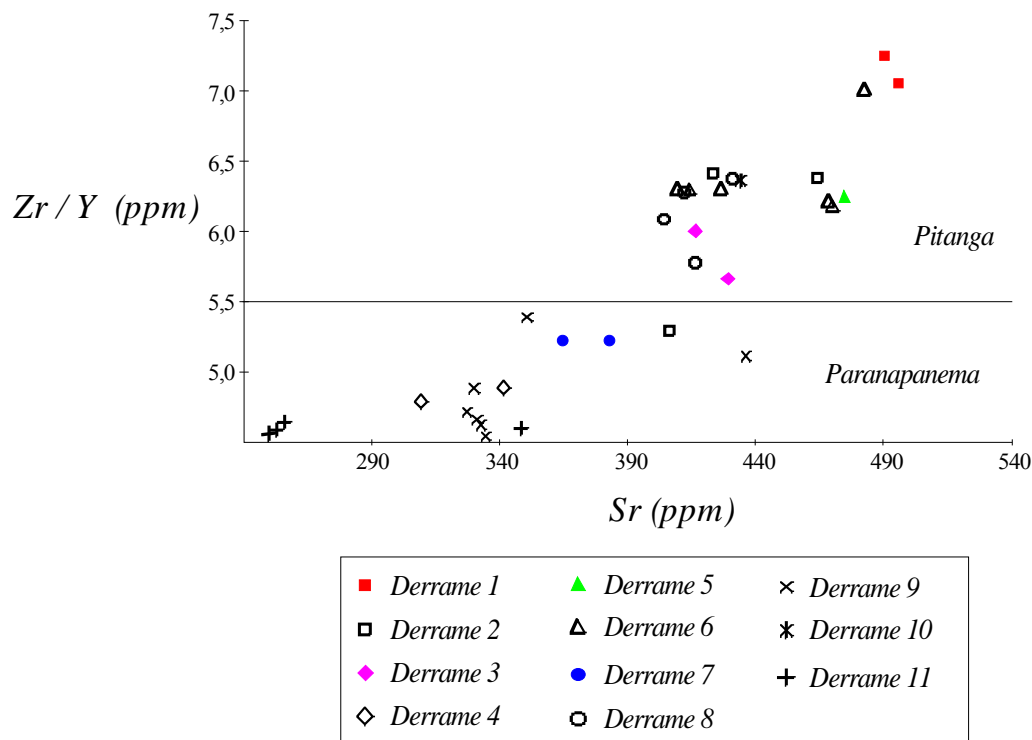


Fig. 3- Variações de Zr/Y e Sr nos derrames da região de Frederico Westphalen. A linha horizontal delimita os campos correspondentes aos tipos Pitanga e Paranapanema (segundo Peate, 1989).

3. A DISTRIBUIÇÃO DAS FASES MINERAIS TARDIAS

Processos descritos de forma genérica como de “alteração” de basaltos são considerados responsáveis pela formação de uma variedade de minerais que ocorrem em um número surpreendente de hábitos, formas, cores e tamanhos. Dentre estes, destacam-se ametistas, zeolitas, calcitas e os argilominerais.

Os argilominerais são principalmente esmectitas e celadonitas e ocorrem em sítios bem definidos na rocha:

- 1 - como substituição de olivinas e, secundariamente, piroxênios e plagioclásios;
- 2 - precipitados nos espaços inter-granulares;
- 3 - preenchendo vesículas e nas bordas de geodos;
- 4 - precipitados nas fraturas.

A origem destes minerais é ainda controversa. Segundo Gomes, 1996, os argilominerais do tipo esmectita encontrados na mesóstase de derrames espessos desta sequência na região são formados por processos tardi-magmáticos, cuja origem está ligada à cristalização direta de um resíduo magmático final enriquecido em sílica e álcalis. Segundo esta autora, a cristalização deste líquido residual dá origem às fases minerais tardias, que se formam após a cristalização magmática ($T < 980^{\circ}\text{C}$), por isso, considerada como cristalização tardi-magmática. O resfriamento muito rápido (“quench”) das lavas submarinas resulta na formação de vidro intersticial, entretanto, a resfriamento comparativamente mais lento dos derrames subaéreos possibilita a cristalização direta do resíduo, originando progressivamente K-feldspato, cristobalita, quartzo e, com o aumento da concentração de H_2O no resíduo, as fases hidratadas como argilominerais e zeolitas.

II – OBJETIVOS GERAIS DO ESTUDO

Dentro do contexto apresentado acima, o presente trabalho tem como objetivo geral o estudo dos argilominerais de um derrame basáltico portador de geodos, procurando estabelecer a gênese destes minerais através da determinação da origem dos fluidos formadores e os processos envolvidos.

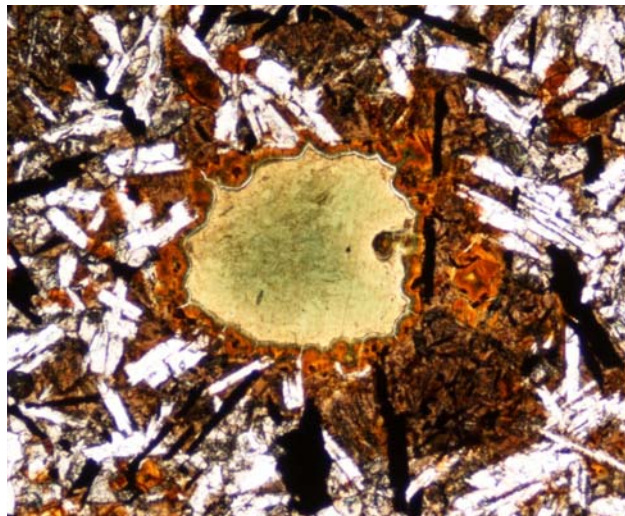
Os objetivos específicos são: - a caracterização dos tipos de argilominerais, suas ocorrências, associações e paragêneses; - o estudo da distribuição dos argilominerais em relação às estruturas do derrame.



UNIVERSIDADE FEDERAL DO RIO GRANDE DO SUL & UNIVERSIDADE DE AVEIRO

Clay studies of Basaltic rocks from the Serra Geral formation in Rio Grande do Sul

Elise Mulocher
M2 IMACS



Summary

I. Introduction	10
II. Local geology.....	11
III. Material and methods.....	17
IV. Results.....	19
1. Macroscopic observations.....	19
2. Optical Microscope.....	20
General aspect of the basalt, reference sample BT.....	20
Evolution of the samples in function of the distance to the Geode.	21
3. XRD analys.	23
4. SEM on rock fragments Images.	25
5. SEM on slides EDS.	27
V. Discussions.	31
1. Macroscopic, fieldtrip interpretation.	31
2. Optical Microscope.	31
3. XRD analysis.	32
4. SEM on rock fragments Images.	33
5. SEM on slides EDS.	34
VI. Conclusions.	35
References.	37
Appendix.	38

I. Introduction

The aim of this master thesis is to study and understand how the clays present in a flow basal deposit could have formed. Two hypotheses can be made: they are either formed by alteration of the magma during time by hydrothermal circulation or either formed during the cooling from the residual lava. In fact, those basalts could be considered as a terrestrial homolog of Mars magmatic activity. So in function of the conclusion made about the Brazilian basalts, a better understanding of the presence of clays on Mars could be achieved.

The basalt flow deposit studied is the 6th of a basaltic sequence of the Alto Uruguai region in the Rio Grande do Sul state. This deposit is situated in the Serra Geral formation which is the Brazilian part of a big geological event: the formation of the Paraná-Etendeka basin. According Hawkesworth et al (1996), the magmatic province of Paraná-Etendeka occurs in early cretaceous and lasted around 11Ma (from 127 to 138Ma). The Paraná covers at least 1.2 million km² over southern Brazil, Uruguay, eastern Paraguay and northern Argentina and reaches a maximum thickness of about 1.7km. This event is contemporaneous and probably linked to the northward opening of South Atlantic Ocean (cf figure 1) and the arrival of the Tristan mantle plume (Gilg et al, 2003). The Parana series can be geochemically divided into two types: high-Ti group with basalts of Pitanga, Paranapanema and Urubici and rhyolites of the Chapeco type; and a low-Ti group with basalts of Gramado, Esmeralda and rhyolites from Palmas type (Gilg et al, 2003). Their eruptions were diachronously, the older lava flows are high-Ti type and mostly in the northwest part and the younger flows are low-Ti in the southeast region. Peate (1997) emphasizes that the different magmas were erupted probably not from the same source and not only due to a lithospheric extension but under both influence of the south Atlantic opening and the interaction plume-lithosphere. This hypothesis is based on the fact that those basalts contains some trace element and isotopic features not commonly observed in oceanic basalts as the depletion of Nb and Ta relative to La and, to a lesser extent of K (Hawkesworth et al, 1992). And also, some major element compositions have been observed requiring a mantle source distinct from an oceanic one.

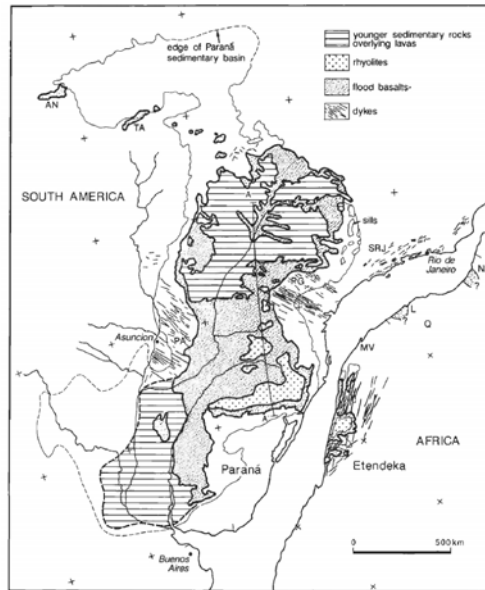


Figure 1: Extension of Parana-Etendeka magmatism in relation to Parana sedimentary basin and proto-Atlantic rift (Peate et al, 1992)

II. Local geology

In the extreme North-West part of Rio Grande do Sul, near Ametista do Sul and Frederico Westphalen (cf figure 2), 12 flows were described in the thesis of Boscato (1996) chemically and in terms of structures. The studied area is about 500km² and the 12 flows have a volume of about 20,000km³ of rock. We can see from the figure 3 that the 6th flow has a thickness of 35m.

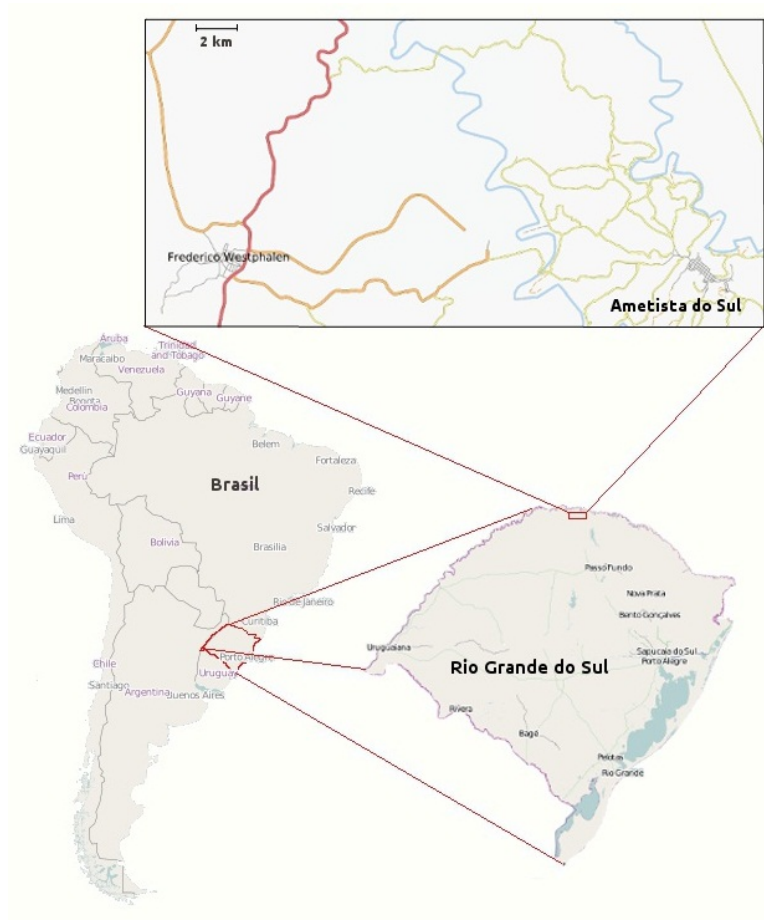


Figure 2: Localisation of prelevement of samples

In the magmatic sequence, two structural aspects were used to differentiate the flow: the presence of vesicles and the fracturation types. Vesicles are the place where were trapped the gas liberated from the magma and they are generally situated in the “solidification front” that limits the top of the lava flow. But a thin layer of vesicles can be observed also at the base. Two types of structural flows have been described by Boscato (1996): type “I” that generally has a thickness of 15 to 35m and the type II that is thicker with an average of 30 to 50m.

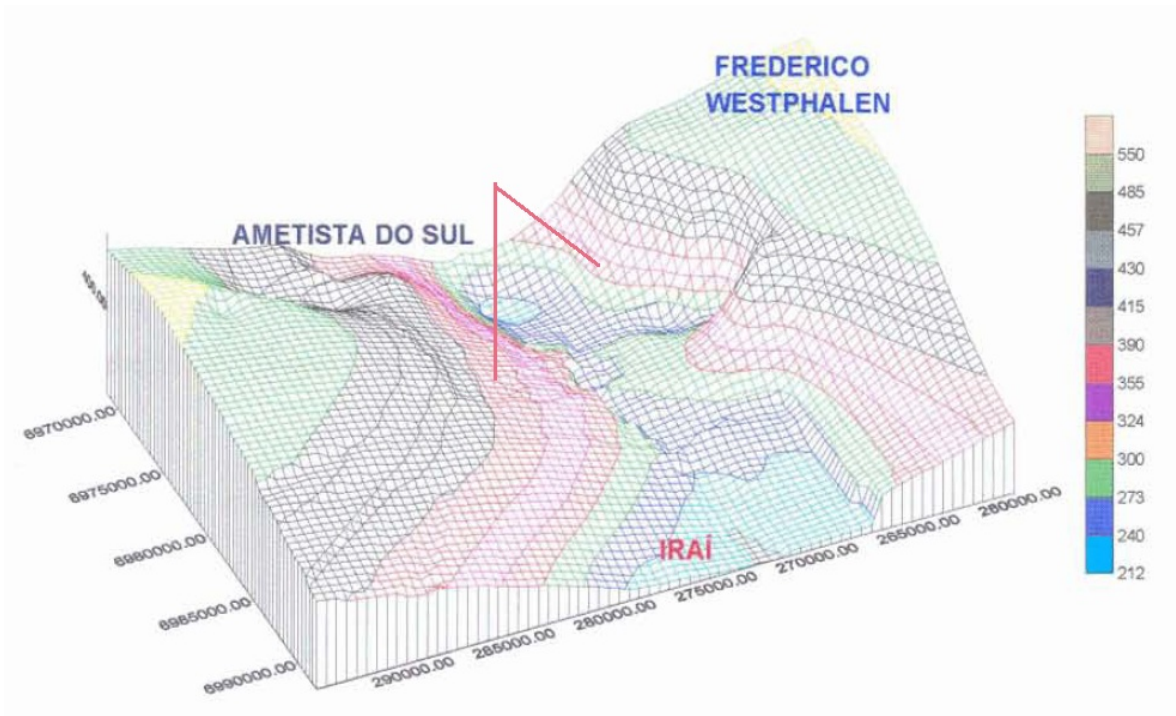


Figure 3: 3D geological map of the 12 lava flows and their respective thickness (Boscato, 1996)

Flows number 2 ,3 ,6 ,7 ,8 ,9 and 10 are from the first type (cf figure 4 and 5) and are constituted as follow:

- a basal level that contains vesicles and generally really thin (50cm in average)
- then, there is a medium level more thick, from 10 to 25m, with a lot of irregular fracturations, not well defined. In the top of this layer, there is an internal macrovesicular level that contains geodes (from few millimeters to few meters diameter). Those geodes are principally filled with silica minerals as amethyst, agate and chalcedony but can also have associated minerals as calcite and zeolites. The top of the medium level is where exploited in order to extract the geodes filled with phenocrystals.
- the superior level, from 2 to 4 m thick, is a massive basalt, without vesicles and with a lot of fractures more horizontally oriented. On the photo (figure 4), we can see that this layer is the top of the galleries.
- and a finally 1 to 2m thick layer where vesicles (from millimeter to centimeter diameter) are filled with zeolites, calcite, quartz and clays.

Other flows (1, 4, 5, 11 and 12) belong to the structural type 2 and are constituted of:

- a basal layer with a thickness from 40 to 100cm, containing vesicles with a rising size toward the top of the layer.

- a massive medium zone (from 30 to 40m thick) divided in three levels differentiating by type of fracturation. The first and the third levels contain vertical fractures (column type) forming prisms of pentagons or hexagons, then fracturation is much more irregular (entablement type).

- a layer with a thickness of 10m containing vesicles filled with quartz, zeolites, calcite and clays (smectite type).

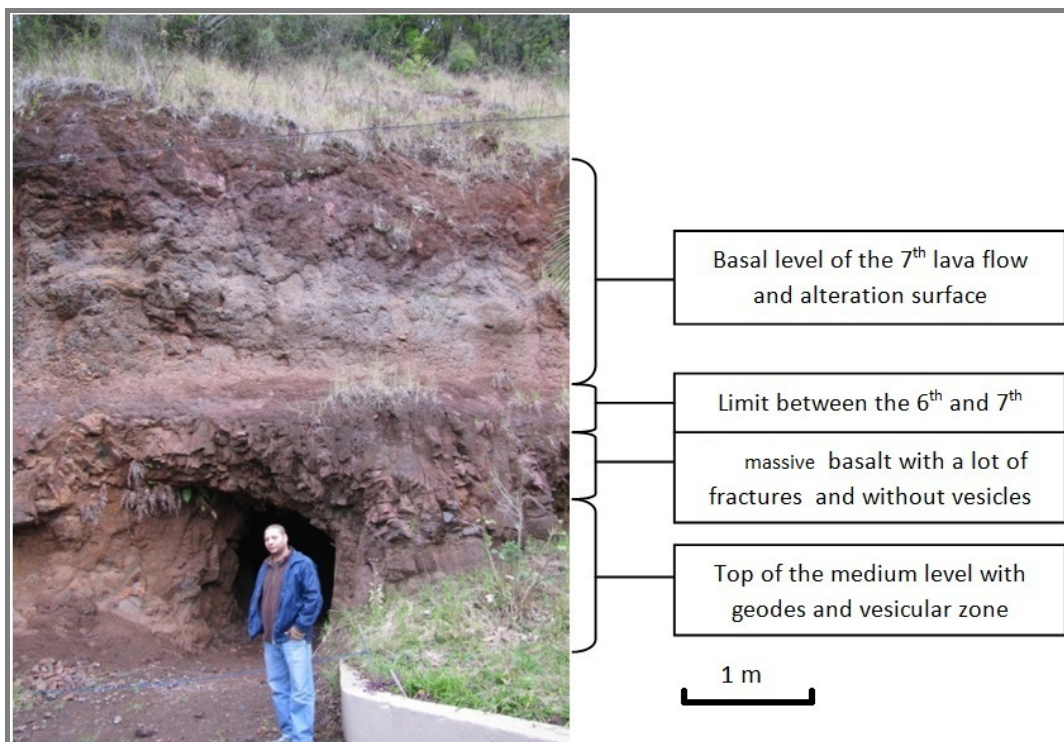


Figure 4: Photo of the exploited zone

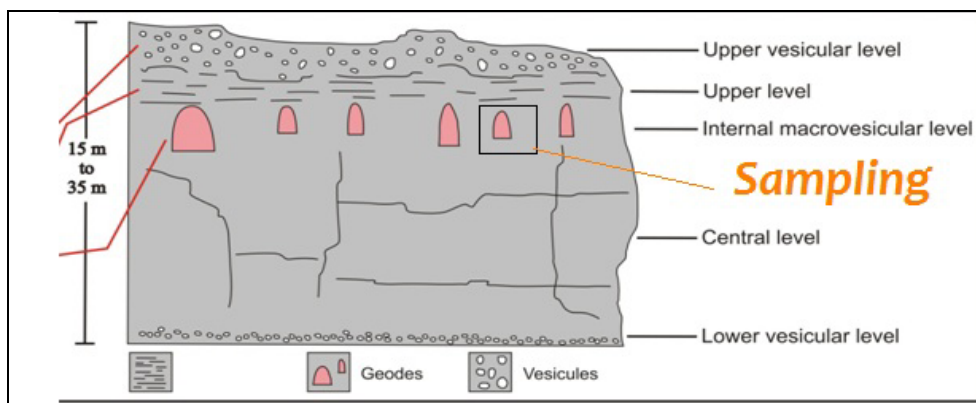


Figure 5: Schema of the structural type 1 (Boscato, 1996)

Mineralogy and texture of lava flows of the type I (that contains the studied flow deposit) is basically the same: phenocrysts and microcrystals of plagioclase (labradorite types), augite, and oxides minerals as magnetite, titanomagnetite or ilmenite, olivines (sparse and completely altered in Fe-Saponite and celadonite in the 6th flow); an acidic mesostasis and some apatites in intergrain spaces.

Texture is intergranular to intersertal in almost all lava flows according to Pinto et al (2011). But in the top of the medium level that contains vesicles and geodes, we can observe a microporphyritic texture only in the regions of large vesicles that generally contains silica geodes (cf figure 6). This zone contains elongated microphenocrysts of plagioclase and augite in a cryptocrystalline matrix.

Those flows contain a lot of clay minerals in intergrain spaces or as an alteration of olivine.

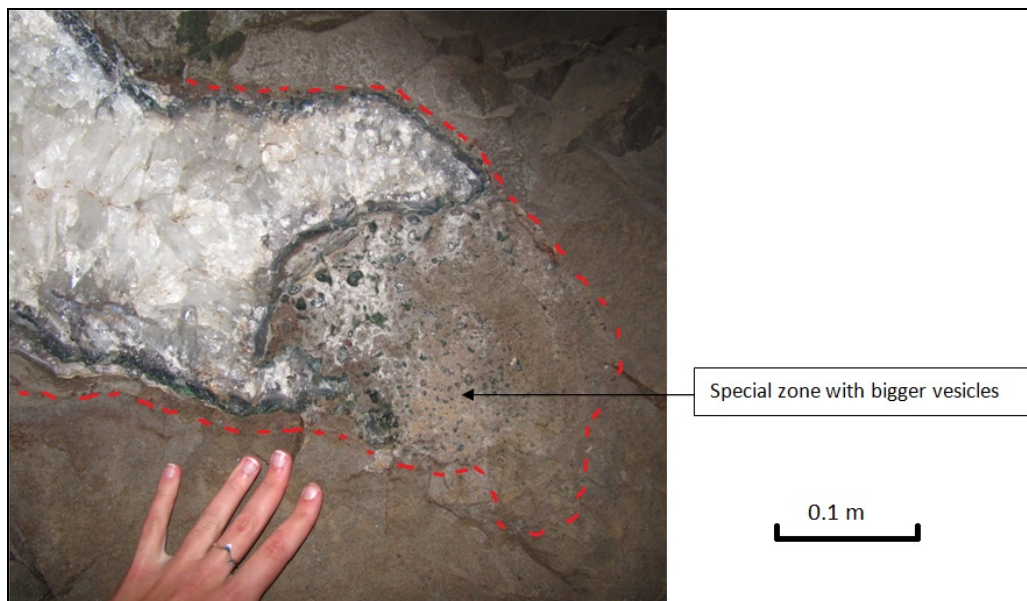


Figure 6: special zone near a geode of amethyst

The chemistry of this sequence was classified by Peate (1992) among a study of the overall Parana basin. With the table 1 below, we can see the different criteria used to differentiate the basalts in terms of chemical composition. In the region of Ametista do Sul, the sequence is only composed of High-Ti basalts according to the different chemical analysis performed by Boscato (1996), as we can observe in the figure 7.

	'High-Ti'			'Low-Ti'		
	Urubici	Pitanga	Paranapanema	Ribeira	Esmeralda	Gramado
SiO ₂	> 49	> 47	48 - 53	49 - 52	48 - 55	49 - 60
TiO ₂	> 3.3	> 2.8	1.7- 3.2	1.5 - 2.3	1.1- 2.3	0.7 - 2.0
P ₂ O ₅	> 0.45	> 0.35	0.2- 0.8	0.15- 0.50	0.1- 0.35	0.05- 0.40
Fe ₂ O ₃ (t)	< 14.5	12.5-18	12.5- 17	12 - 16	12 - 17	9 - 16
Sr	>550	>350	200 -450	200 -375	<250	140 -400
Ba	>500	>200	200 -650	200 -600	90 -400	100 -700
Zr	>250	>200	120 -250	100 -200	65 -210	65 -275
Ti/Zr	> 57	> 60	> 65	> 65	> 60	< 70
Ti/Y	>500	>350	>350	>300	<330	<330
Zr/Y	> 6.5	> 5.5	4.0- 7.0	3.5 - 7.0	2.0- 5.0	3.5 - 6.5
Sr/Y	> 14	> 8	4.5- 15	5 - 17	< 9	< 13
Ba/Y	> 14	> 9	5 - 19	6 - 19	< 12	< 19

Table 1: Classification criteria for basalt magma types (Peate et al, 1992)

The ancient classification of “High-Ti Basalts” is divided into three groups called Urubici, Pitanga and Paranapanema. Pitanga and Urubici groups have the highest TiO₂ contents and incompatible trace elements abundances (Hawkesworth et al, 1992). At similar MgO contents, Urubici contain higher SiO₂, TiO₂, K₂O and lower Fe₂O₃ than Pitanga. Moreover, Urubici abundance of trace elements is the same as Pitanga but a higher content. Elements that permit to distinguish them clearly are Sr (lower for Pitanga) and Fe₂O₃. Intermediate-Ti samples were classified in the group called Paranapanema. They can be distinguished from Pitanga by their lower TiO₂ contents but they have basically the same Fe₂O₃ content and the same other elements at a lower content according Peate (1992).

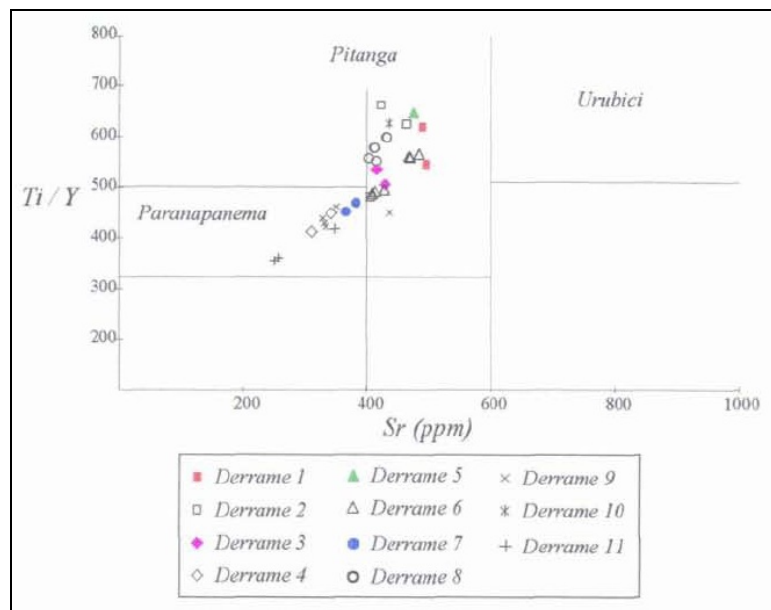


Figure 7: lava flows in function of their magmatic type defined here by variations of Ti/Y and Sr (Boscato, 1996)

The 6th flow deposit belongs in the figure 7 to the Pitanga magmatic group, so its chemical composition is close to the one describe for Pitanga in the table 1.

What we want to understand is the origin of the clay minerals and there place in the rock (matrix, vesicles, intergrain spaces etc...) in this deposit. So, we are going to speak first the methods used and the different samples. Then, present the results and finally try to interpret and discuss them.

III. Materials and methods

The 8 samples were taken from the 6th flow of a basaltic sequence of the Alto Uruguai region in Rio Grande do Sul state. Seven samples were taken in the level containing the amethysts geodes from different distances of one geode selected (cf figure8) in a mine belonging to Bortoluzzi. And a reference sample BT was taken in the massive part under the geodes level. The geode near the sampling area had a diameter of 40*50cm and the samples were taken as follow: BT4 65 cm from the geode, BT3 50 cm, BT2 35 cm, BT1A and BT1B near the geode wall. Sample BT1A for the microscope slide was containing a part of the special zone with bigger vesicles.

D7 is another sample used in chemical analysis and X-ray diffraction that come from another mine but from the same flow deposit. It is composed of fine green clay particles directly taken from a big vesicle.

From samples BT1, the special zone has been separated using dentist's tool as well as the filling of the big vesicles. This creates two new samples called "special zone" and "celadonite" for X-Ray diffraction and chemical analysis.

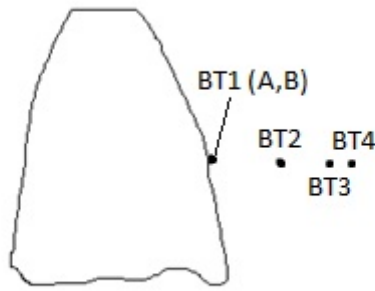


Figure 8: Demonstration of prelevment of samples

For this project, different methods of analysis have been used.

First of all, macroscopic and microscopic observations were done for each sample using a magnifying glass and an optical microscope with natural and polarized light for the slides.

Two samples, BT1A and BT3, have been powdered in order to make X-Ray diffraction (XRD) pattern of the bulk rock. Then, a separation of the fraction smaller than $2\mu\text{m}$ was done using the centrifugation method and the Stokes' law. It allows to make oriented slides and ethylene glycolation of the finer fraction and to identify clay particles. D7 was separated using Stokes' law and decantation in a less than $10\mu\text{m}$ fraction in order to eliminate mostly others minerals as quartz for example. On this sample and "Celadonite", oriented slides and glycolation were done. A powder of the special zone was realized and an extraction of the minor $2\mu\text{m}$ part was done to realize an oriented slide. And finally from small samples BT, BT4 and BT2, we attempt to make powder and then separate the minor $2\mu\text{m}$ fraction in order to make diffraction patterns (cf results chapter). The XRD machine used was a SIEMENS D5000 of the University of Porto Alegre with a copper filament. This device allows us to measure the beam reflected by the crystal in order to characterize it or to characterize its atomic scale structure. But the detection limit of the phases is about 3% for mixed materials so a low quantity of minerals can't be detected.

Secondary electron images (SEM) show morphology and topography of a sample. The more the number of electrons reaching the detector, the brighter the image is. This technique was used to provide images of rock samples. On the SEM, back scattered electron (BSE) images can be done coupling energy dispersive spectroscopy(EDS) analysis, to provide images and chemical analysis. BSE shows

difference in composition - or more exactly, difference in atomic number over a sample. The higher the atomic numbers of the atom, the more backscattered electrons are bounced back, making the image brighter for larger atoms. BSE images are very helpful for obtaining high-resolution compositional maps of a sample and for quickly distinguishing different phases. An EDS detector is used to separate the characteristic x-rays of different elements, produced by the interaction of an electron beam on the surface of the sample, into an energy spectrum. An EDS system software is used to analyze the energy spectrum in order to determine the abundance of specific elements. EDS can be used to find the chemical composition of materials down to a spot size of a few microns, and to create an element composition maps over a much broader raster area.

In Portugal, SEM was performed for images with a tungsten filament (Hitachi S4100) and in Brazil, two SEM were used: a JEOL JSM6060 for images and a JSM5800 for EDS analysis and chemical map. For images, small pieces of samples were chosen and covered with gold in order to make the sample surface electrically conductive and electrically grounded to prevent the accumulation of electrostatic charge at the surface. It is because nonconductive specimens tend to charge when they are scanned by the electron beam, and especially in secondary electron imaging mode, this causes scanning faults and other image artifacts. Additionally, coating may increase signal/noise ratio for samples of low atomic number.

EDS and chemical maps were done on the slides previously observed at optical microscope and coated with carbon instead of gold to avoid superposition of gold peaks among others in chemical spectrum.

IV. Results

1. Macroscopic observations

For the reference sample BT, the rock is darker than the others. Vesicles are not clearly visible without microscope. It is a basic magmatic rock, with some phenocrystals and a dark mesostasis. Others samples are clearer, with the presence of vesicles smaller than a millimeter but no clear difference is visible while going toward

the geode. In the BT1A sample, we can see a special zone, which seems to contain mainly mesostasis and where we can find vesicles of a bigger size (appendix 1) from the millimeter to few meters as the geodes exploited by the Galimpo.

2. Optical Microscope

We want to compare the differences in texture, mineralogy degree of alteration etc... of the reference sample: BT and samples from BT4 to BT1. We are going to show observations for the reference sample and the general aspect of the basalt, and then describe the evolution of aspect of primary minerals and textures.

- **General aspect of the basalt, reference sample BT**

- Texture

The slide is dark unaided-eyes and in the microscope. We can differentiate three types of crystal by their size: phenocrystals (from about 300 μm to several millimeter), microcrystals of less than 300 μm and mesostasis (glass material and/or very fine crystallized material). Phenocrystals and microcrystals are not preferentially oriented. The rock also contains vesicles and intergrain spaces filled with different layers. The texture of the rock can be described from intergranular (with interstices between plagioclase grains filled by pyroxenes, iron titanium oxides and some rare olivines) to intersertal texture (interstices are occupied by glass or cryptocrystalline material).

- Mineralogy

Phenocrystals are mainly automorphs but with traces of alteration (fractures, oxide inclusions etc...) and composed of three main types:

-crystal with a low refringence and a low birefringence (first order), automorph tabular with polysynthetic twinning characteristic of a Feldspar. It has extinction at about 70°. So this mineral is probably a plagioclase (Na-Ca feldspar), as we can see in appendix 2.

-a crystal with a high relief, sometime automorph, sometime with a prismatic shape. The crystal has a refringence in the yellow-green of the first order and a medium birefringence with sometimes pleiochromism in function of the orientation of the crystal. This mineral is a pyroxene and is often fractured in the samples (appendix 3).

-an oxide with an elongated shape, black in LPNA and LP, characteristic of an oxide as magnetite or hematite (appendix 4).

Microcrystals contain the same minerals plagioclase, pyroxene and oxides (appendix 5). The mesostasis is dark, greenish and seems sometime altered to a brownish dark colors. It sometimes has a fibrous shape that make think that it contains clay minerals (appendix 4 and 6).

Sometime, a strange mineralization can be observed. Its size is like phenocrystals size. It seems to have a composition similar to the mesostasis but with a bright orange color and with a lot of oxides intercalated (appendix 7).

- Vesicles and intergrains

The vesicles in this slide have an average size under 300 μ m and have originally a circular shape but can be deformed because of the coalescence effect (appendix 8). Intergrains are smaller and angular because they fill the space between the phenocrystals and microcrystals. They can even isolate a mineral (appendix 9). Both filling are the same. The border is composed of an orange fine grains matrix, larger for the smaller vesicles or intergrains (about 10 μ m wide) probably composed of clay minerals. And the middle is filled with yellow-green fine minerals or sometimes the filling seems to have disappeared maybe due to a strong polishing so the difference of color can be link to the thickness of the clays.

- **Evolution of the samples in function of the distance to the Geode**

- BT4

The slide is clearer than the reference sample. The mineralogy is the same for every sample. Phenocrystals are also fractured. Some pyroxenes have an orange zonation in non polarized and polarized light which is an alteration in iron oxihydroxides (appendix 10).

Vesicles have the same filling as the reference sample. But sometime, we can observe filling with more layer (appendix 11) that we have to observe by SEM later to be able to distinguish clay species.

Sometime, we can observe an orange zone containing a lot of oxides, which could be an intergrain space altered, a vesicle or an entirely altered primary mineral as for example olivine (which are not common in this basalt).

- BT3

The slide is as clear as BT4. The filling of vesicles is different for this sample. We only observe an orange filling that seems to be more homogeneous and the size of vesicles seems to be smaller. There is also a zone where the mesostasis is bigger (appendix 12). The mesostasis seems to be filled with very fine fibrous minerals and clays because of the color and the stripes.

- BT2

In this sample, the vesicles are similar to the ones from BT3, with only an orange filling but they are a bit bigger (appendix 13).

We can observe the presence of more alteration trace of primary minerals than in the previous samples. Macrocristals are fractured and with inclusions of oxi-hydroxides (red spots appendix 14). Furthermore, those oxi-hydroxides can be present in pyroxenes and mesostasis (appendix 15).

- BT1 A

This slide is darker than the previous ones but clearer than the reference sample. It's can be explain by the degree of alteration more important of this. Here, vesicles are mainly filled with green fine mineral (appendix 16) generally with a fine darker border. There is an orange layer around vesicles but that doesn't seem to be inside the vesicles and therefore due to an alteration that occurs around the vesicles as a filling of intergrain spaces (appendix 17).

- BT1 AA

The slide is generally darker and altered than the other slides (but still less than the reference sample). Macrocristals are more altered and feldspar are not completely white, but yellowish with oxi-hydroxides. In this zone, vesicles are similar as BT1A

This slide has a special zone that we can see by the eye, where macrocristals and vesicles are bigger (between 2 to 7mm).

The texture of the special zone is different (appendix 18): there is no macrocristals, only microcristals and mesostasis. There is a lot of oxide minerals with a different shape from the normal zone, they are more quadratic. We can also observe feldspar and pyroxenes all elongated and small (about 70microns). A fibrous mineral is

also observed, sometimes bigger than feldspar and pyroxenes minerals, dark in natural light and orange with a low birefringence in polarized light. This mineral seems to be composed or altered in clays due to his color and because it seems to contains a lot of oxides inclusions.

The mesostasis contains sometime green zonations and others with orange and red spots.

In this zone, vesicles are bigger and filled with a more deep green mineral. They contains almost no orange layer around but we can see a vacuum due to a strong polishing of the slide. There is different shades of green here too (appendix 19).

We can observe the limit between the two zone which is quite well defined in the appendix 20.

- **BT1 AB**

The slide is darker than the ones more far from the geode but clearer than other BT1. Vesicles are similar to the two previous ones with sometime different shades of green (appendix 21).

We can observe again the orange zone with small vesicles inside (appendix 22) that can emphasize an intergrain space filling more than the alteration of an olivine.

There is a zone where all the pyroxenes have the same orientation (no brightful color) which can represent the flow movement of the magma.

3. XRD analysis

First, a powder of the bulk rock of the samples BT, BT4, BT3, BT2 and BT1A (appendix 23) were made. But for samples BT, BT4 and BT2, the amount of rock used was really low and can explain the bad quality of the XRD pattern for their powders and the less than 2μ part (not enough quantity of particles). We can see that the different samples contain two types of feldspar: anorthite (position peak by intensity: 3.2, 3.18 and 4.04\AA) in bigger relative quantity than the K feldspar characterized by the three main peaks: 3.29, 3.24 and 4.22\AA (for microcline). We can also observe augite, a clinopyroxene (1.43 , 1.62 and 2.99\AA), some iron oxide that can be either hematite (2.69 , 1.69 and 2.51\AA) or ilmenite (2.75 , 2.54 and 1.72\AA) and more clearly in BT3 and BT1A

we can see smectite that according to the data base is characterized by a montmorillonite containing iron (15, 4.5 and 5.1Å).

The less than 2 μ part of each sample shows more clearly that every sample contains smectite (appendix 24). The peak is more defined. In almost all samples, anorthite peaks are still visible as well as hematite peak. That can be due to the break of particles during the crushing of the sample before the separation. In the sample BT1A, we can see a peak at around 10Å that corresponds to the d001 of celadonite and other peaks at 2.58, 4.53 and 3.64Å. Because during the preparation, it was impossible to find a part of the rock without vesicles (i.e. without celadonite). We are going to see more in details the XRD patterns of the samples BT3 and BT1A.

The powder diffraction of BT3 (appendix 25) shows a well defined crystallization of anorthite and augite. We can observe also small broader peaks of iron oxides containing titanium as ilmenite or only iron like hematite. And the oriented slides measured natural (Air Dry AD) and with ethylene glycol (EG) show a shift of the peak from 15.3 to 16Å that confirms the presence of smectite type clays.

The powder diffraction of BT1A (appendix 26) shows the same mineral of the bulk rock and a peak of smectite a bit higher better defined as in the sample BT3. A peak at 2.56Å is characteristic of the d004 of celadonite but the d001 is invisible at 10Å. The oriented slide shows also the shift of smectite peak while glycolated and a peak at 10Å that confirms the presence of celadonite but in small quantity compared relatively with the size of the peak of smectite.

XRD pattern of the special zone (appendix 27) shows a similar pattern as the environmental rock. It contains anorthite, K feldspar, augite, iron (titanium) oxides and smectites. But we can also observe a peak that corresponds to quartz (3.34 and also 4.25 and 1.81Å), the d004 of celadonite and some small peaks that could correspond to apatite (2.77, 2.86 and 1.83Å). The oriented slide of the less than 2 μ m part shows a broad peak of smectite and the d001 peak of celadonite.

The diffraction pattern of the vesicles contained within the special zone reveals shows very thin and well defined peaks of celadonite (appendix 28). Furthermore, we can observe the presence of the peak of quartz probably due to the presence of a filling of silica mineral in the bigger vesicles that was removed with the celadonite during the

extraction. Sample D7, which comes from a large vesicle of green clays, contains celadonite well crystallized and quartz (appendix 29) as for the celadonite in the previous appendix. We can also notice a broad peak at 15.3\AA that shifts to 16.3\AA with glycolation and characterizes the presence of a small amount of smectite.

4. SEM on rock fragments Images

On all the samples, we could observe phenocrystal alteration, but every time the growing of smectite doesn't seem to depend of this alteration. As we can see in figure 8 and appendix 30, phenocrystals of feldspar are altered in function of their clivages and twinned but there is no growing of clays on this surface, and in the first appendix we can see that smectite has grown on the border.

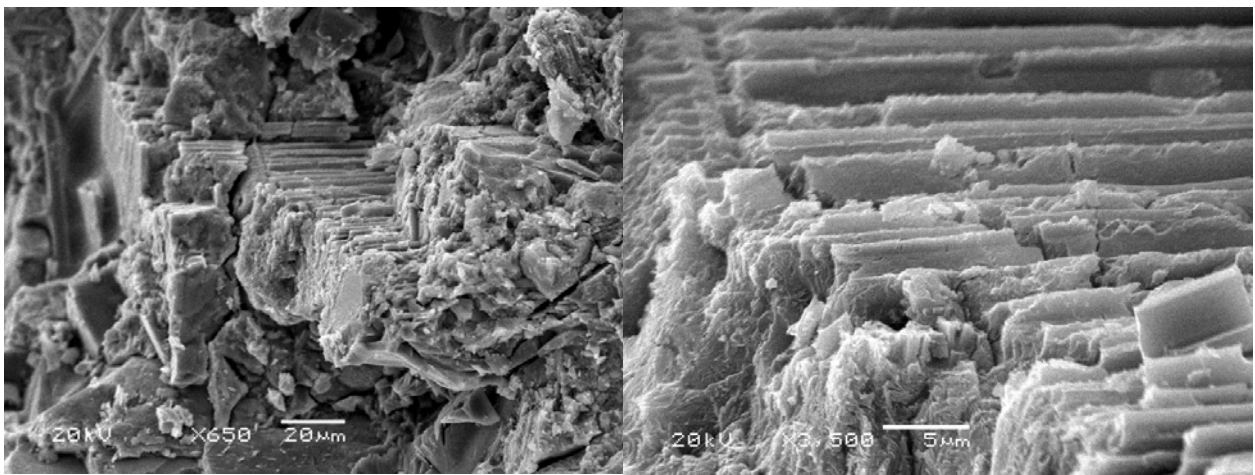


Figure 8: Alteration of a feldspar

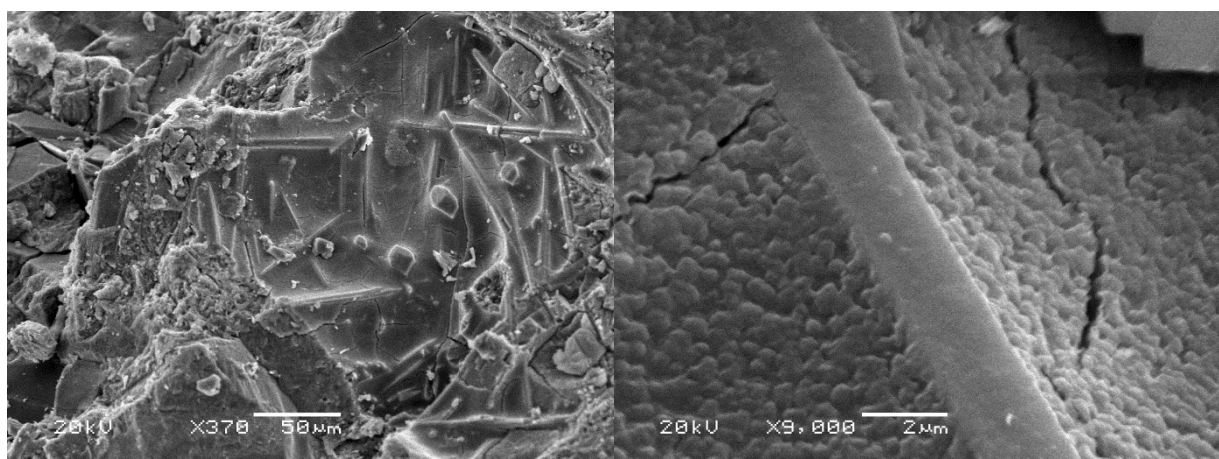


Figure 9: zones of alteration with clays and oxides

Smectite shape in samples is quite well crystallized and parallel to the phenocrystals (appendix 31).

Zones of alteration and mesostasis observed in microscope have been seen in the SEM (appendix 32 and figure 9). They are composed of oxides and a matrix composed of clay minerals, probably smectite.

Vesicles (appendix 32) have been observed with three generations of clay minerals, a thin layer of about 5 μ m of smectite as observed previously, a layer thicker of about 30 μ m with elongated clays that are probably celadonite and in the middle of the vesicle again small clay minerals that looks more like smectite.

Well crystallized apatite can be observed in the rock (appendix 33).

In the special zone, (appendix 34) smectite is well crystallized as in the bulk rock.

Vesicles contain also different generations of clay minerals. On the external part again a 5-10 μ m layer of smectite (appendix 35), then there is a layer of 30-40 μ m of celadonite and another time a microcrystal layer of clay mineral probably more smectitic from the shape and finally a silica layer (cf figure 10). Some crystallization of celadonite can be observed sometime inside the vesicles (appendix 34).

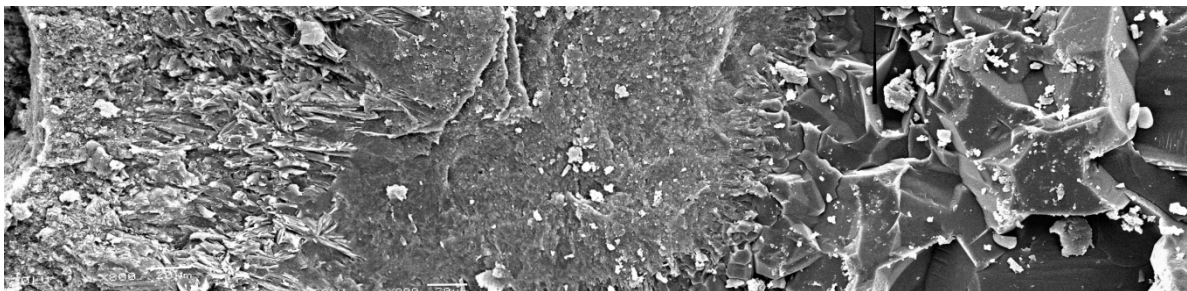


Figure 10: composition of a vesicle from the outside to the inside (left to right)

The mesostasis seems to contain mainly oxides and clay mineral that are in a particular shape. (appendix 36). Apatite can be observed in a bigger amount in the mesostasis (appendix 37). Here they seem to be partly dissolved.

5. SEM on slides EDS

Chemical analysis and also chemical maps have been done on the slides previously observed with the optical microscope. Chemical analysis from EDS methods can't be quantified because the precision wasn't sufficient. But it can give an idea of the elements composing the minerals and therefore we can guess minerals from the shape and the chemical composition.

Results will be presented as follow: macrocrystals chemistry, mesostasis composition, differences of composition of vesicles from different samples and finally the chemical composition of the special zone and its vesicles.

- Macrocrystal chemistry

In the appendix (appendix 38), we can see that phenocrystals of feldspar are composed of sodium and calcium (with some oxyhydroxide). So that confirms the XRD pattern of the presence of anorthite. Microcrystals have also the same composition (appendix 39).

Pyroxene crystals contain calcium, magnesium, iron, aluminum and some sodium (appendix 39), so they are augite type. In the appendix 38, a macrocrystal of augite contains the same elements but with the presence of potassium. This crystal is completely altered, with fractures filled with oxides and clays. From the appendix 39, we can observe crystals of oxides composed with 50% of titanium and 50% of iron which is characteristic of ilmenite.

- Mesostasis composition

Composition of mesostasis is slightly different from the macrocrystals. Feldspar composition tends more to a potassic system as we can see in appendix 40. But the composition of augite remains the same with the presence again of some potassium. In the mesostasis, we can also observe some clay. In the sample BT1AA closer to the geode, we can also observe apatite in form of hydroxyapatite.

- Vesicles in BT4

Two types of vesicles can be observed in this sample. The ones that contain only smectite clay are generally smaller (less than 500microns). The smectite contains iron, calcium, magnesium and aluminium (appendix 41).

The other type of vesicles, bigger than 500 microns, contains the same minerals as the first type (smectite) and probably some celadonite due to the presence of potassium. We can see that in the border of the vesicle, EDS detects only calcium but going toward the center, we can observe the presence of small quantity potassium (figure 11 and table 2).

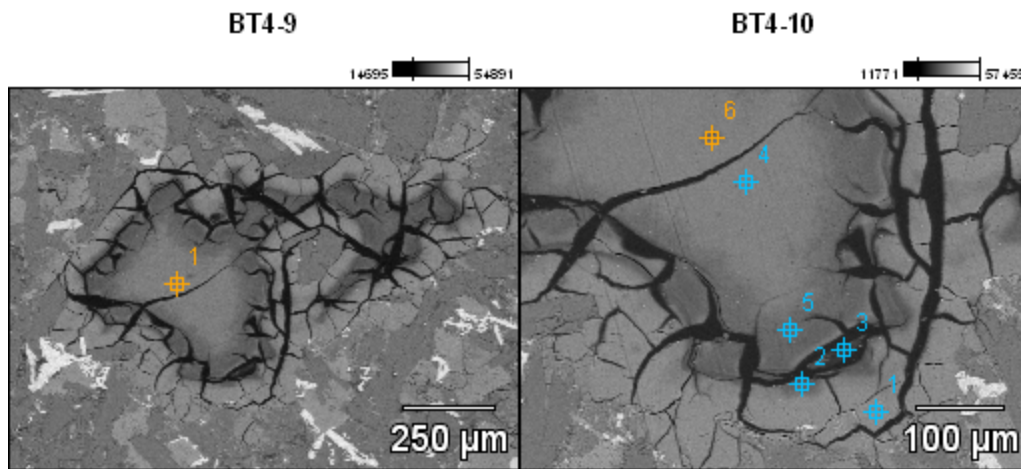


Figure 11: chemical analysis of a vesicle

Compound %

	<i>O</i>	<i>Mg</i>	<i>Al</i>	<i>Si</i>	<i>K</i>	<i>Ca</i>	<i>Fe</i>
BT4-10_pt1	12.48	8.25	5.85	32.49		5.44	35.49
BT4-10_pt2	12.04	6.15	5.93	36.49		4.92	34.48
BT4-10_pt3		5.74	4.22	45.98		5.90	38.15
BT4-10_pt4	9.65	6.17	5.29	40.15	1.32	3.47	33.96
BT4-10_pt5	11.63	6.09	6.97	41.71	1.26	4.47	27.87
BT4-10_pt6	12.65	5.72	5.89	38.79	1.31	5.74	29.89

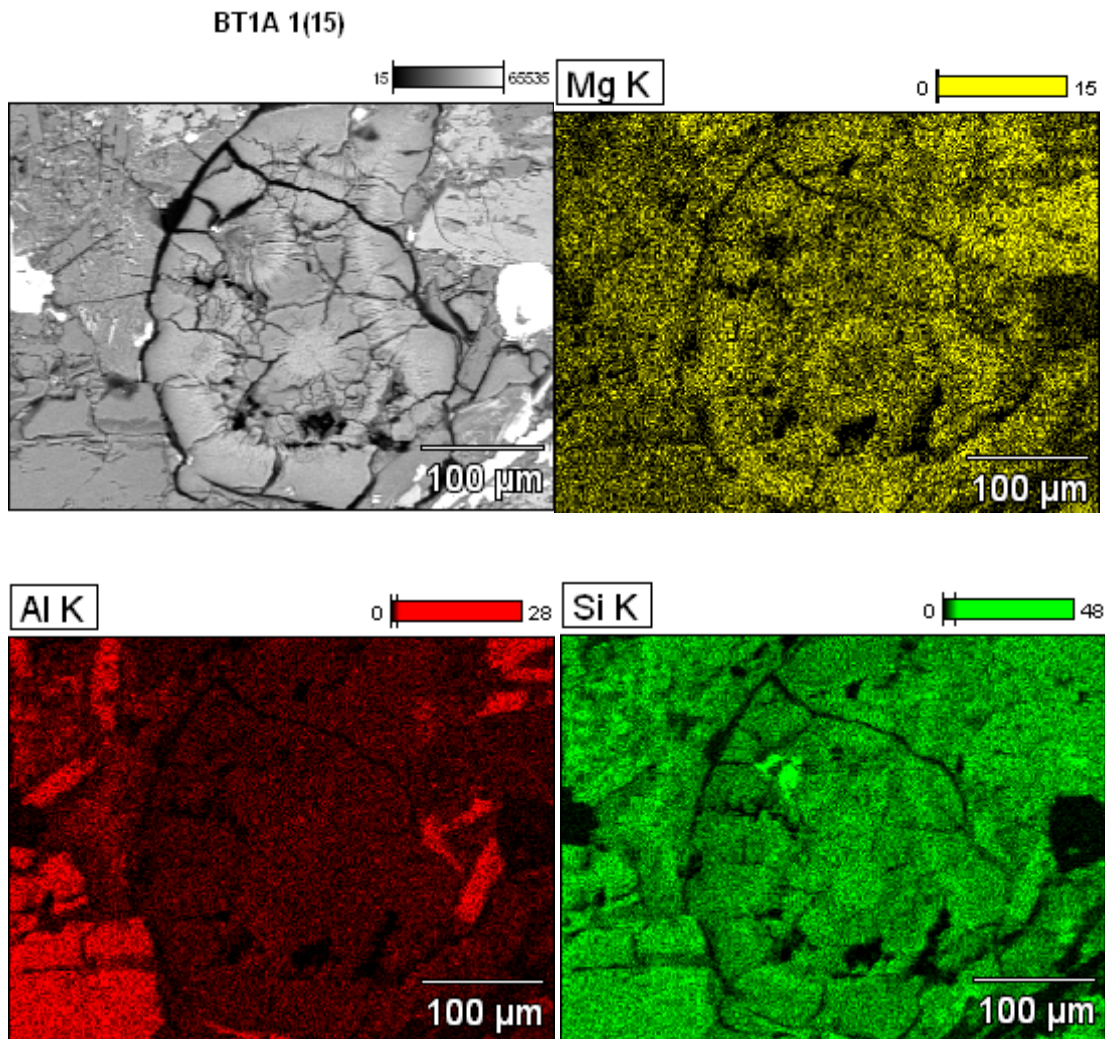
Table 2: Chemical elements of the different points mesured

- Vesicles in BT2-3 with only smectite

The same type of vesicles as in BT4, containing potassium, can be observe (appendix 42).

- Vesicles in BT1

We can observe vesicles of the second type also, containing potassium. But a clearer after the border is more rich in potassium as we can see in the three examples (figure 12 , appendix 43 and 45).



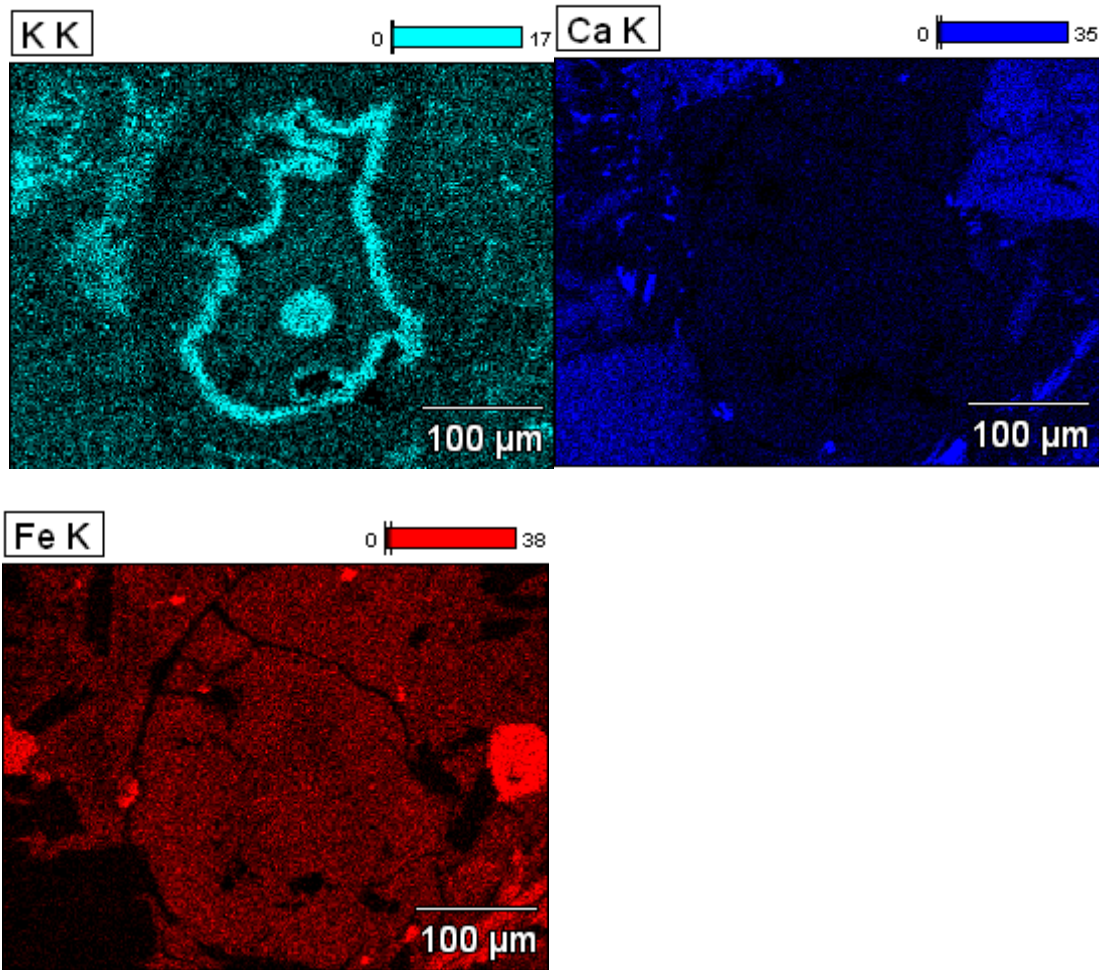


Figure 12: chemical map of a vesicle

In the normal zone, we can also observe some apatite, containing phosphor and calcium so probably hydroxyapatite type (appendix 44). Moreover, it was also observed in the mesostasis in form of microcrystals.

- Special zone

The mesostasis of the special zone contains the same minerals as the general rock, but a lot more of apatite crystals can be seen (appendix 46).

- Vesicles in the special zone

Vesicles of the special zone are bigger, but have a similar composition as the smaller ones. The chemical map show the presence of calcium in all the vesicle but the presence of potassium more toward the center with again a line with a high concentration of potassium a bit after the border of the vesicle. But the point technique shows different concentrations of calcium (appendix 47).

- Comparison of two types of oxides (appendix 48)

We can see that the shape of oxides in the special zone is more hexagonal whereas the ones in the normal rock are more elongated. Chemical composition is also slightly different for the distribution of titanium and iron. In the small oxide, the ratio is about 1/4 and for the elongated mineral 1. So in the special zone, oxides are mostly titanomagnetite while in the rock, they are mostly ilmenite.

V. Discussions

1. Macroscopic, fieldtrip interpretation

We can observe that the special zone is always linked to the big silicate geodes and seems finer on the border of the vesicles and like a tail on each side. For a more precise observations, we need a microscope.

2. Optical Microscope

We have three generations of crystals: macrocrystals, microcrystals and the mesostasis. So the texture is from intergranular to intersertal. That can be explained by two steps of cooling, one in the magmatic chamber where the phenocrystals have grown, the climb up where microcrystals have grown and then, the eruption where the mesostasis formed and were bubbles of gas get fixed.

We can see that phenocrystals and microcrystals are automorph and that the filling of the intergrain spaces fit around so we can think that the filling is post crystallization. Some vesicles are completely circular shape (appendix 8) and some others are deformed and look like a mix of vesicles and filling of intergrain spaces. So we can think that the bubbles of gas were present from the beginning, during the growing of crystals and that probably they were moving up to the top of the lava flow and agglomerate together which can explain the strange shape of certain intergrain spaces and the presence of vesicles only in a certain part of the lava flow.

There is also two types of filling, an orange filling which is probably smectite and a green filling which corresponds to celadonite. Smectite is around the vesicles, as a thin layer but because the limit of the vesicle is not well defined we can't determine if

smectite has grown in the vesicle before the growing of celadonite or if it has grown around the vesicle, as a reaction of the mesostasis or as an alteration process. By the shape of smectite in the SEM and their chemical analysis, we can maybe describe better their origins. Celadonite is always present only in the vesicles. Moreover, sometime we can see different shade of green, to yellow-green so we can think that there are probably different generations of celadonite in the vesicles.

Furthermore, some places of the mesostasis seem to contain clays which are dark green-brown and in other place more orange (ferrous). We can think that the mesostasis contains also clay minerals which are probably smectites but we are not able from those observations to say if they are due to an alteration of the mesostasis or were formed from the residual magma flow. And the orange alteration that sometime has a shape of an ancient mineral (appendix 22) could be a result of the complete alteration of olivine into oxides and clays.

The texture of the special zone is cryptocrystalline with microphenocrystals that are elongated. And the vesicles in this zone seem to contain less smectite or it has maybe disappear during the polishing.

Now, the question is when the filling of vesicles and intergrain spaces occur. We have to understand if the clays were formed during the cooling or by hydrothermal alteration of the basalt.

3. XRD analysis

XRD patterns confirm that reference sample and the others have the same mineralogy: feldspar (alkali and plagioclase), augite, oxides, smectite. Celadonite is only detected on BT1A but the powders of BT2, BT4 and BT were done on a very small amount and therefore less precise.

Comparison of BT1A and BT3 patterns shows that BT1A seems to contain more smectite because the peak has a higher intensity and is thinner. that can be explain by a better crystallization of the minerals.

The special zone shows peaks of quartz and celadonite that can be explain by the pollution of some vesicles present in the special zone during the extraction by the

dentist tool. Some peaks could correspond to the one of apatite. That means that apatite is in quite big quantity compared to the normal rock. The peak of smectite is quite big and seems to be the addition of two peaks at around 15 and 15.5Å. This could be because of different hydration state of smectites.

Diffraction pattern of vesicles in special zone show the presence of a very well crystallized Celadonite and in quite big quantity. Presence of quartz is due to the secondary filling of the vesicles. No smectite were detected because the border of vesicles was not extracted to avoid contamination of the rock. In appendix 27, we can see a very small peak of smectite that could correspond to the orange border of the vesicles seen on microscope.

XRD results correlate the previous observations and seem to show that there is an evolution of the composition of vesicles from the distance to the geode or maybe the quantity of celadonite contained with the vesicles were under the detection limit of the apparatus for the samples.

4. SEM on rock fragments Images

Smectite shape is well crystallized, parallel to phenocrystals and doesn't grow in the alteration zones. This observation enhances the hypothesis of a clay mineral growing during the cooling and not from a later alteration.

The ferrous zones observed in microscope are composed of clay minerals (smectite) and oxides. They are probably a zone where the mesostasis is thicker or an intergrain filling.

Vesicles seem to contain different generations of clay minerals with a first one of smectite, a second of celadonite and a last one with smectite again.

Apatite is observed in both zones but more numerous in the special zone. It can be an indication of a differentiation of this magma if it is more concentrated in poor elements. But this has to be observed in chemical analysis.

Special zone contains vesicles with silica filling as the big geodes extracted in the mine. And the mesostasis of this zone is mainly composed of smectite well crystallized.

5. SEM on slides EDS

EDS analysis confirm the previous mineralogy and give some precisions about the species of minerals. Macrocrystal feldspar are mainly anorthite type, with a composition that place the mineral in the labradorite group. But microcrystals of feldspar contain more K that means that they are plagioclases with sometime some sodium. Pyroxenes are augite types with an empirical formula $\text{Ca}_{0,9}\text{Na}_{0,1}\text{Mg}_{0,9}\text{Fe}_{0,2}\text{Al}_{0,4}\text{Si}_2\text{O}_6$. Presence of potassium in this quantity in a pyroxene is impossible so it can either be due to an error of the EDS measurement because of a mineral near containing potassium as a feldspar or by an error of calibration of the probe that could explain also the presence of potassium in smectite layer of the vesicles. We have to observe results from microprobe. The two types of oxides are titanium-iron oxide $\text{Fe}^{2+}\text{TiO}_3$ (ilmenite) and iron oxide $\text{Fe}^{3+}_2\text{Fe}^{2+}\text{O}_4$ (magnetite).

The change of type of feldspar from macrocrystal to microcrystal minerals can be explained by the enrichment of the magma in potassium during the crystallization of macrocrystals. Because pyroxene takes preferentially calcium and feldspar takes calcium and sodium. So relatively, the quantity of calcium and sodium decrease compare to potassium.

The mesostasis composition is the same with augite, potassic feldspar and oxides. We can also see some clay minerals as smectite (but as the pyroxene with a measurement of some potassium). And closer to the big geode, in BT1 and BT1A, we can observe a lot of hydroxyapatites with the empirical formula $\text{Ca}_5(\text{PO}_4)_3(\text{OH})$.

Smectite composition is close to saponite with an empirical formula: $\text{Ca}_{0,1}\text{Na}_{0,1}\text{Mg}_{2,25}\text{Fe}_{0,75}\text{Si}_3\text{AlO}_{10}(\text{OH})_2 \cdot 4(\text{H}_2\text{O})$.

Two types of vesicles were observed, the one that contains only smectite and the one that has alternation of smectite/celadonite. Because generally the ones that contains only smectite were the smaller, we can think that smectite were present before. In the other type of vesicles, the problem is the detection of a small quantity of potassium even if it is a smectite. But from the images provided by the SEM (figure 12, appendix 43 and 45), microscope images (appendix 6 and 11) and with those results, we can think that there were at least three generations of clays: a first one of smectite, a second one of

celadonite and a third one probably of smectite. Vesicles in the special zone belong to the second as seen in SEM (appendix 47) and in EDS analysis.

Here again, we can observe apatite in the special zone and in the rock closer to the geode.

The presence of the special zone around the vesicles could be explained by a bigger size of vesicles, which that means a bigger quantity of gas and as a consequence a faster cooling than in the bulk rock. But if it's a reaction of cooling, we should observe a proportional zonation around bigger vesicles whereas in (figure 6) we can see that the special zone is very fine on the border of the vesicles and form as a tail at the end.

Another explanation is that bigger vesicles could come from a different magma flow from the bottom. Because of the gas and maybe a more fluid composition, the bubbles went up, bringing a bit of the fluid. This hypothesis could explain the elongated shape of the geodes and the presence of a fine border of special zone and at the end a larger tail. And a different chemical composition of this zone as the presence of a relative higher amount of apatite could enhance the fact that the rock of this zone come from a different flow.

Proust et al (2007) emphasize that there is no evidence of hydraulic fracturing at the bottom of geodes. The layer of celadonite covering the wall of the geode is explained in this article as the initial, non-fracturated basaltic wall altered in celadonite by hydrothermal fluids trapped in the geode. This context would also explain the shape of the geode, due to a "higher cooling rate of the basaltic magma at the centre of the geode base in contact with large vapor volume than the magma at the periphery where the contact with volume vapor is more limited and radiating heat loss is smaller" (Proust et al, 2007).

VI. Conclusions

Vesicles in the special zone and normal zone are both composed of celadonite and smectite, sometime with different generation of layers. But vesicles in the special

zone have a bigger size and seem richer in celadonite. The chemical composition of the zone around geodes seems to be slightly different. Because of its shape, the difference of crystallization and composition, the special zone seems to provide from another flow, probably brought by bigger vesicles during the climb up in the magma series.

Previous studies and observations made emphasize the fact that the presence of smectite and celadonite inside smaller vesicles and around geodes wouldn't depend on a hydrothermal alteration in a fractured context but more on an exsolution of gases in a non-fractured system.

But more analysis would precise the origin of the clays. A chemical analysis of the rock couple to the modal analysis of the slides could show if clays are part of the residual magma or if they have an external origin. Furthermore, microprobe analysis could give more details about the different layers of vesicles and about the repartition of potassium. Maybe a more detail study about oxide minerals could also give more information about the origin of the special zone.

References

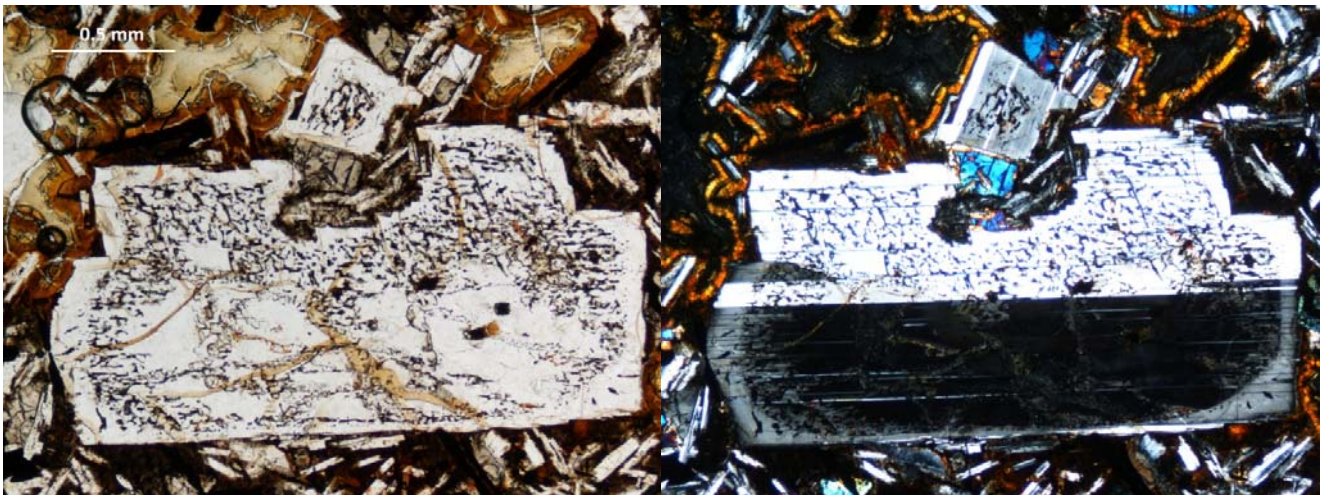
- Boscato Gomes, M E, mecanismos de resfriamento, estruturação e processos pos-magmaticos em basaltos da bacia do parana- regio de Frederico Westphalen (RS)-Brasil, PhD (1996)
- Gilg, H Albert, Giulio Morteani, Yuri Kostitsyn, Christine Preinfalk, Istvan Gatter, and Adedir J Strieder, 'Genesis of Amethyst Geodes in Basaltic Rocks of the Serra Geral Formation (Ametista Do Sul, Rio Grande Do Sul, Brazil): a Fluid Inclusion, REE, Oxygen, Carbon, and Sr Isotope Study on Basalt, Quartz, and Calcite', *Mineralium Deposita*, 38 (2003), 1009-1025.
- Hawkesworth, C J, K Gallagher, S Kelley, M Mantovani, D W Peate, M Regelous, and others, 'Parana Magmatism and the Opening of the South Atlantic', *Magmatism and the Causes of Continental Breakup*, ed. by B C Storey, T Alabaster and R J Pankhurst, 68 (1992), 221.
- Hawkesworth, Chris, Kathy Stewart, Simon Turner, Simon Kelley, I Linda, and Marta Mantovani, 'Basalt Province', *Science*, 143 (1996), 95-109.
- Peate, D W, C J Hawkesworth, and M S M Mantovani, 'Chemical Stratigraphy of the Paraná Lavas (South America): Classification of Magma Types and Their Spatial Distribution', *Bull Volcanology*, 55 (1992), 119-139.
- Peate, David W, 'The Parana-Etendeka Province', *Atlantic*, ed. by J Mahoney and M Coffin, 100 (1997), 217-246.
- Pinto, Viter, and Léo Hartmann, 'Epigenetic Hydrothermal Origin for the Copper Mineralization in the Vista Alegre District , Paraná Volcanic Province , Southernmost Brazil', *Geophysical Research Abstracts*, 13 (2011), 3883-3883.
- Proust, Dominique, and Claude Fontaine, 'Amethyst-bearing Lava Flows in the Paraná Basin (Rio Grande Do Sul , Brazil): Cooling , Vesiculation and Formation of the Geodic Cavities', *October*, 144 (2007), 53-65

Appendix

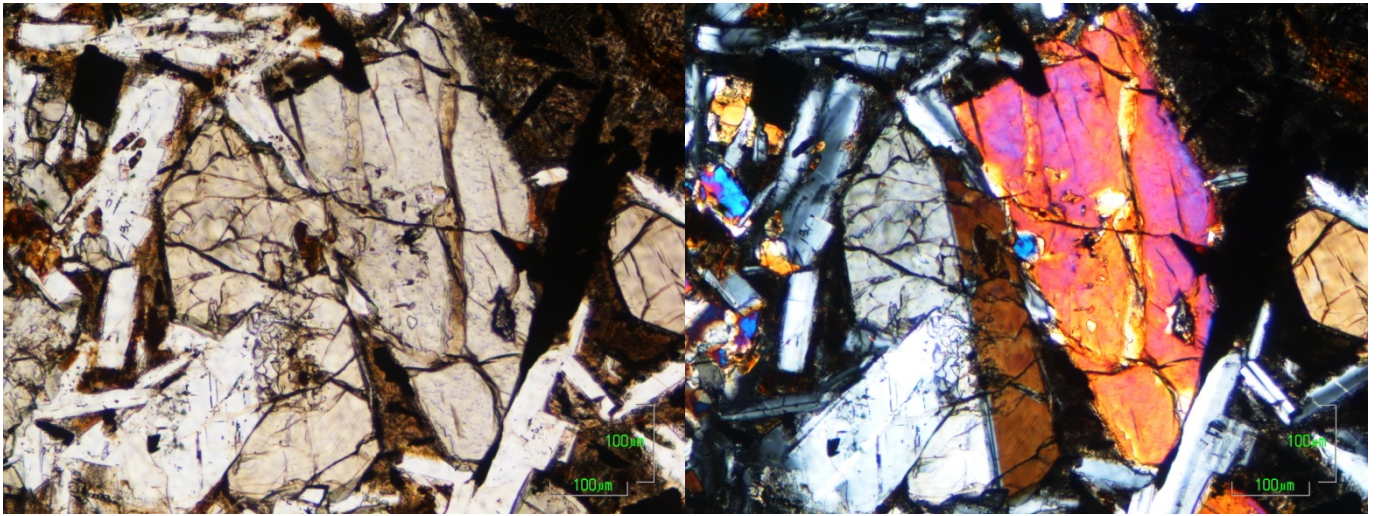
Appendix 1: sample near a big vesicle



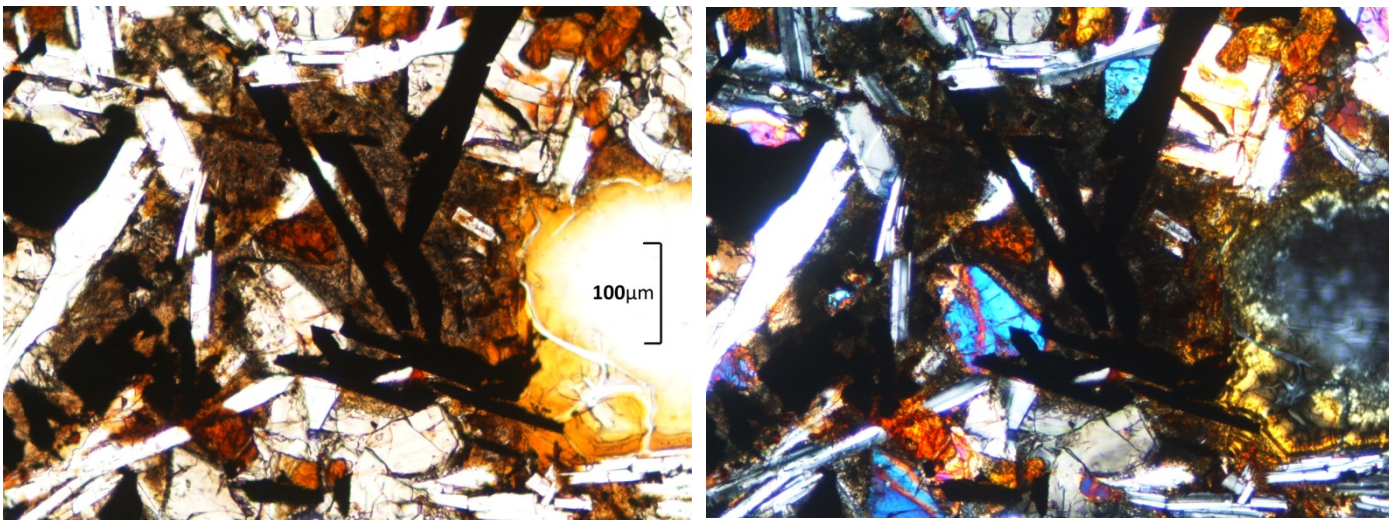
Appendix 2: Feldspar phenocrysts observed in optical microscope (natural and polarized light), sample BT2



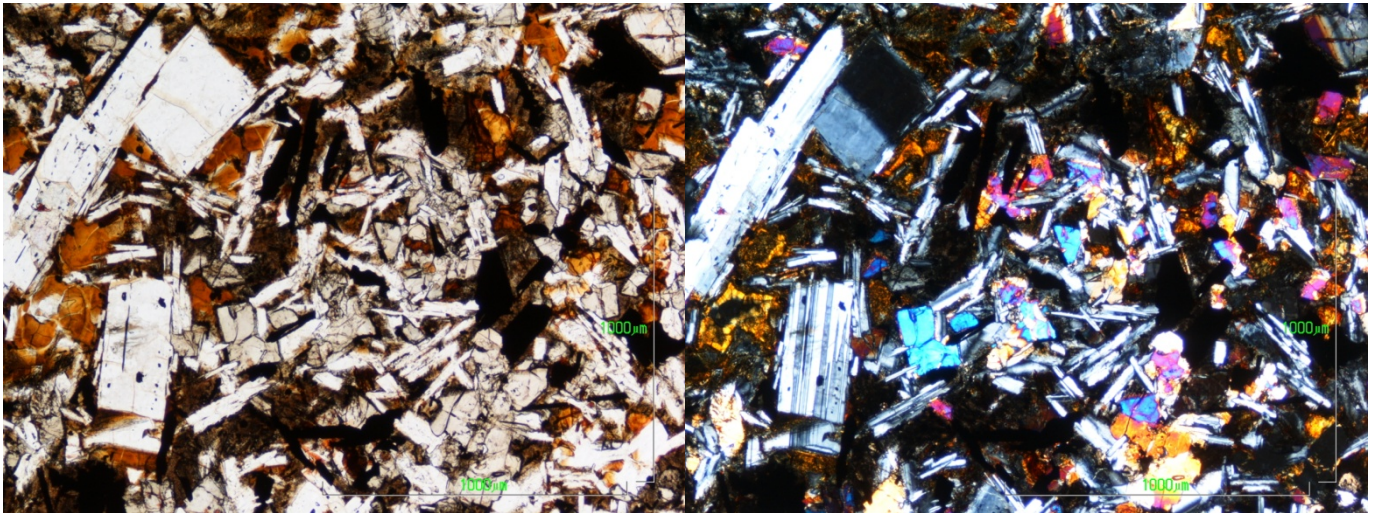
Appendix 3: pyroxene phenocrysts observed in optical microscope (natural and polarized light), sample BT3



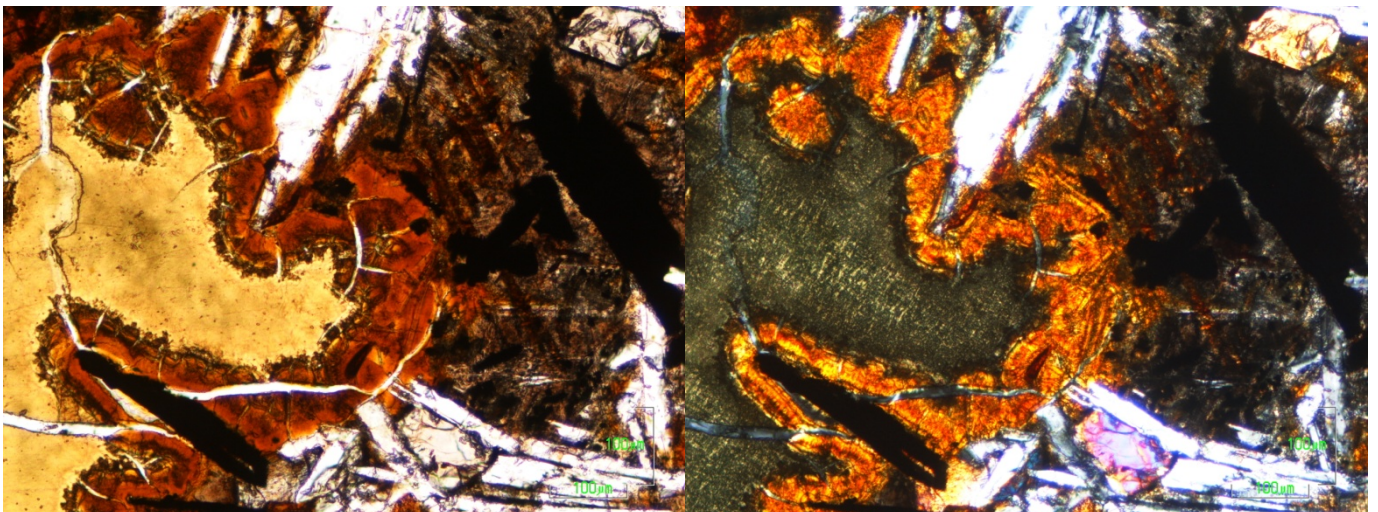
Appendix 4: oxide phenocrysts observed in optical microscope (natural and polarized light), sample BT3



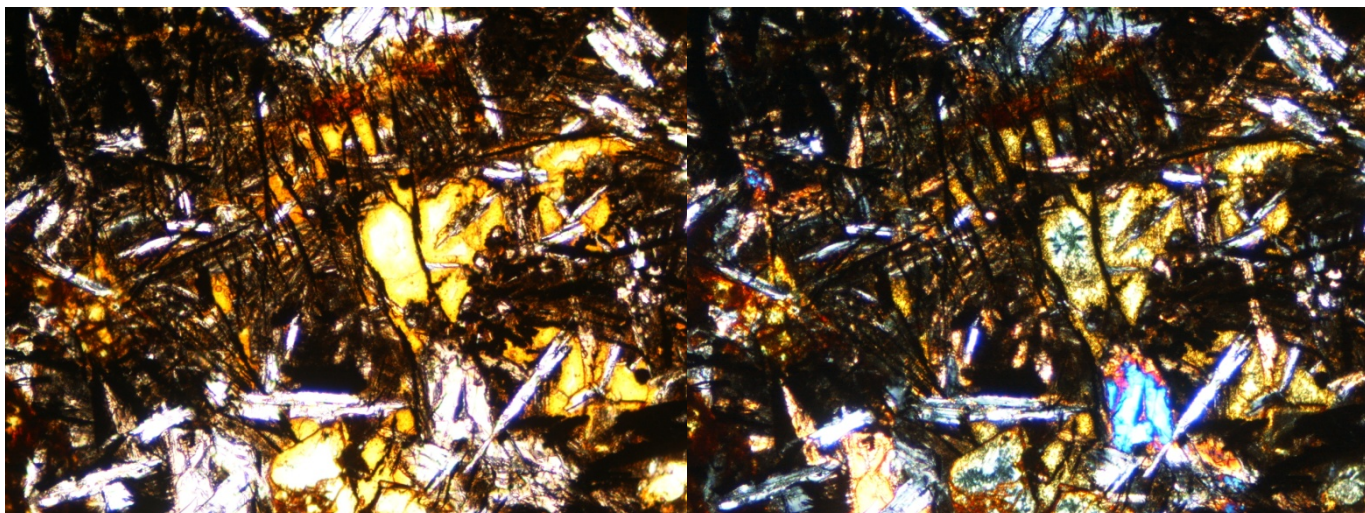
Appendix 5: microcrystals observed in optical microscope (natural and polarized light), sample BT3



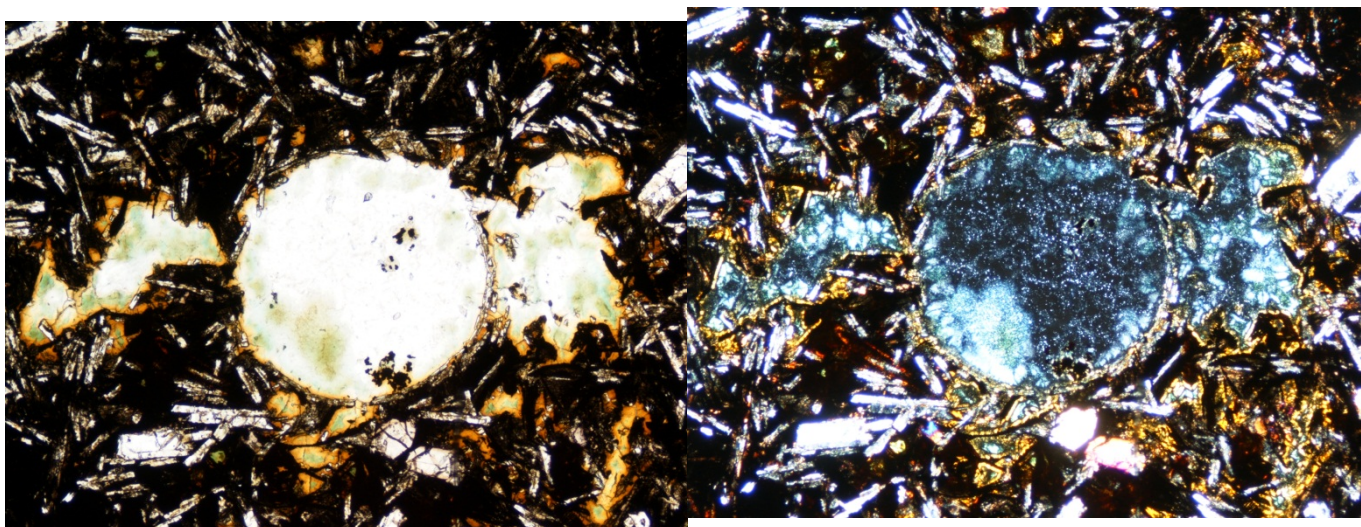
Appendix 6: mesostasis observed in optical microscope (natural and polarized light), sample BT4



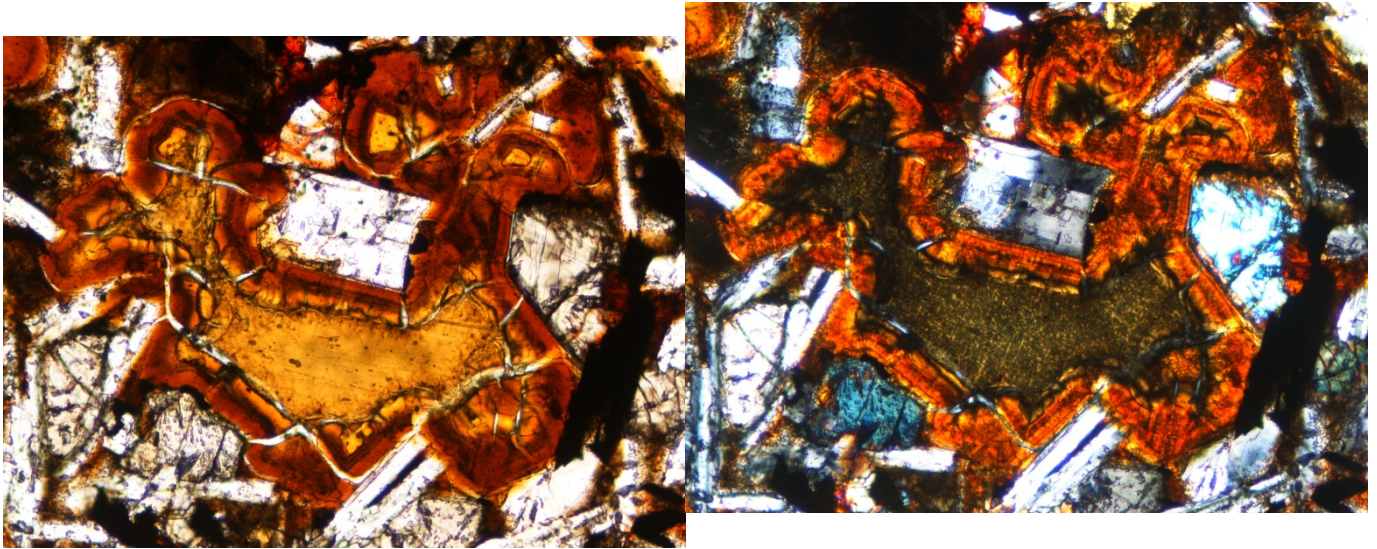
Appendix 7: oxides intercalated with mesostasis and intergrain filling (natural and polarized light), sample BTS



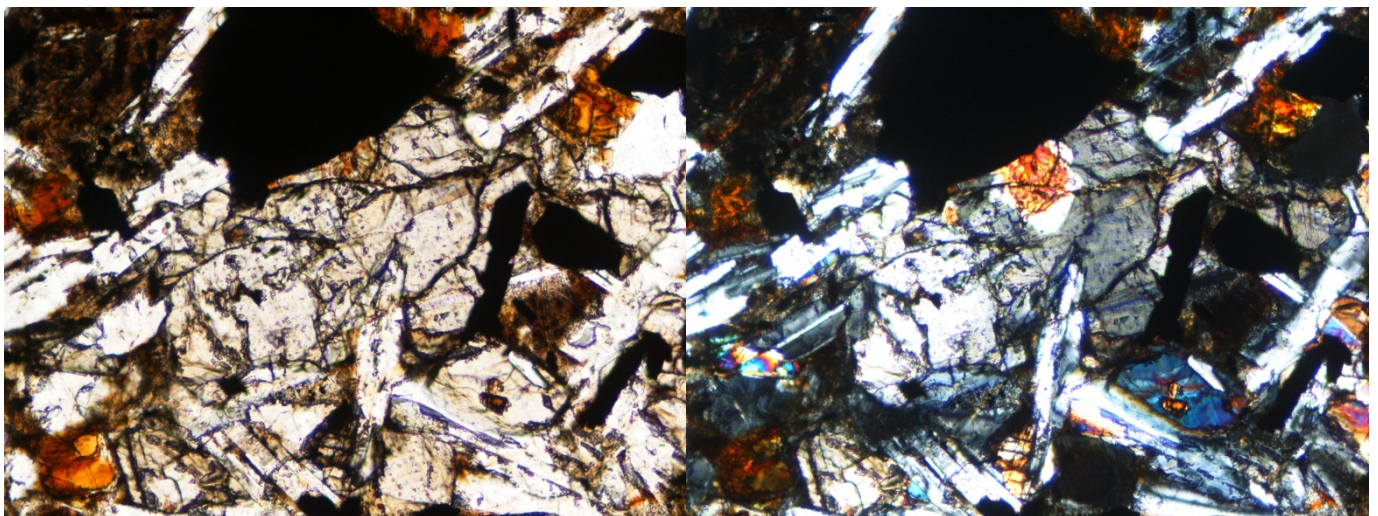
Appendix 8: vesicles and intergrain spaces (natural and polarized light), sample BTS



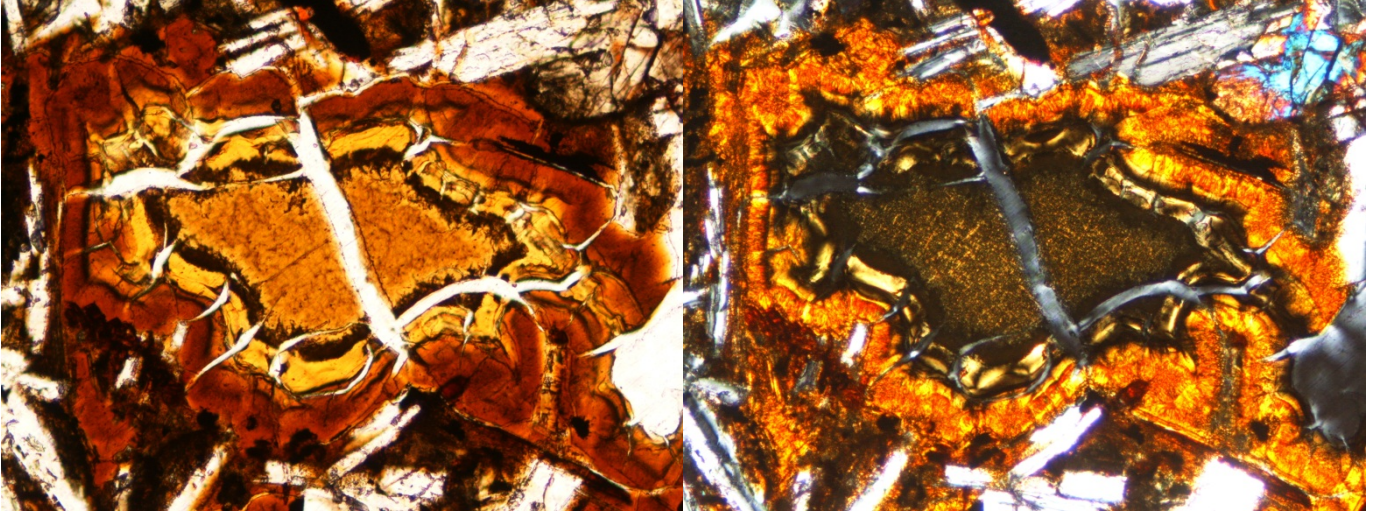
Appendix 9: vesicles observed in optical microscope (natural and polarized light), sample BT4



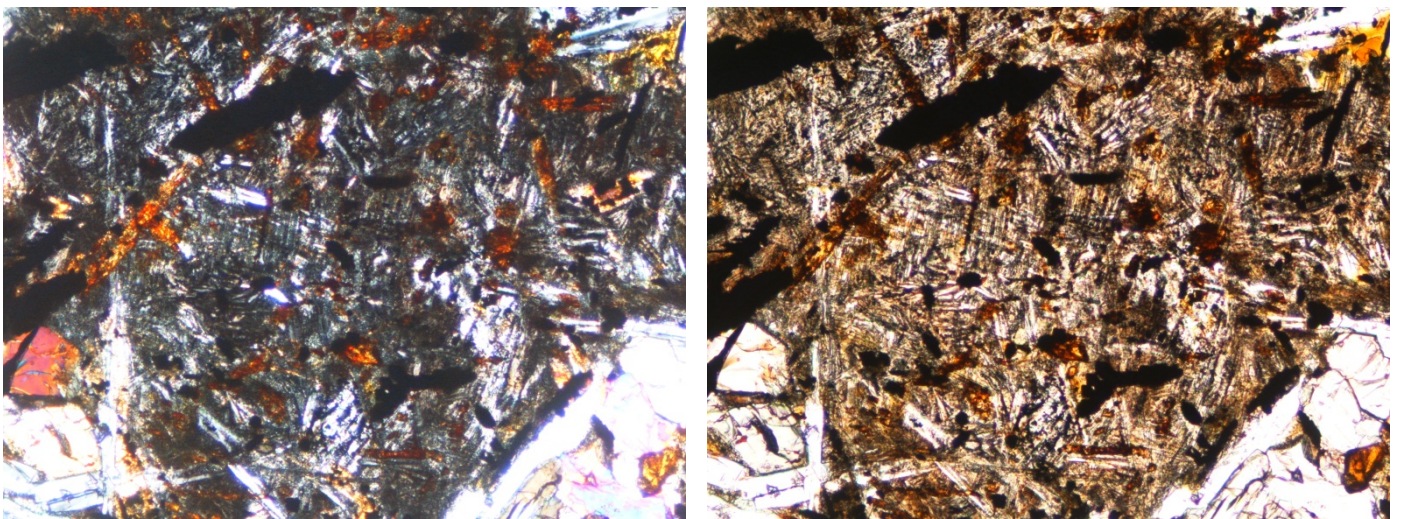
Appendix 10: alteration of a pyroxene in oxyhydroxides (natural and polarized light), sample BT4



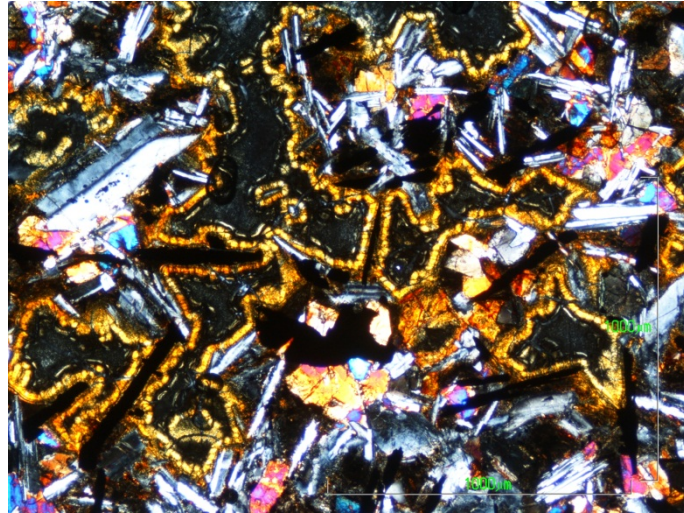
Appendix 11: vesicles filled with four distinct phases (natural and polarized light), sample BT4



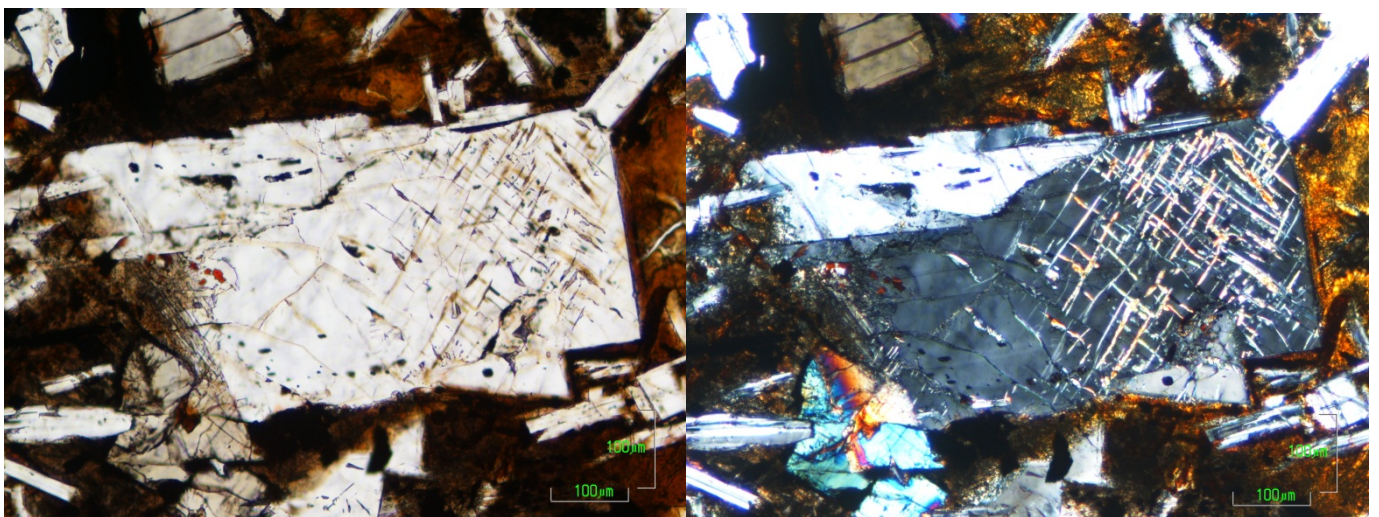
Appendix 12: mesostasis observed in optical microscope (natural and polarized light), sample BT3



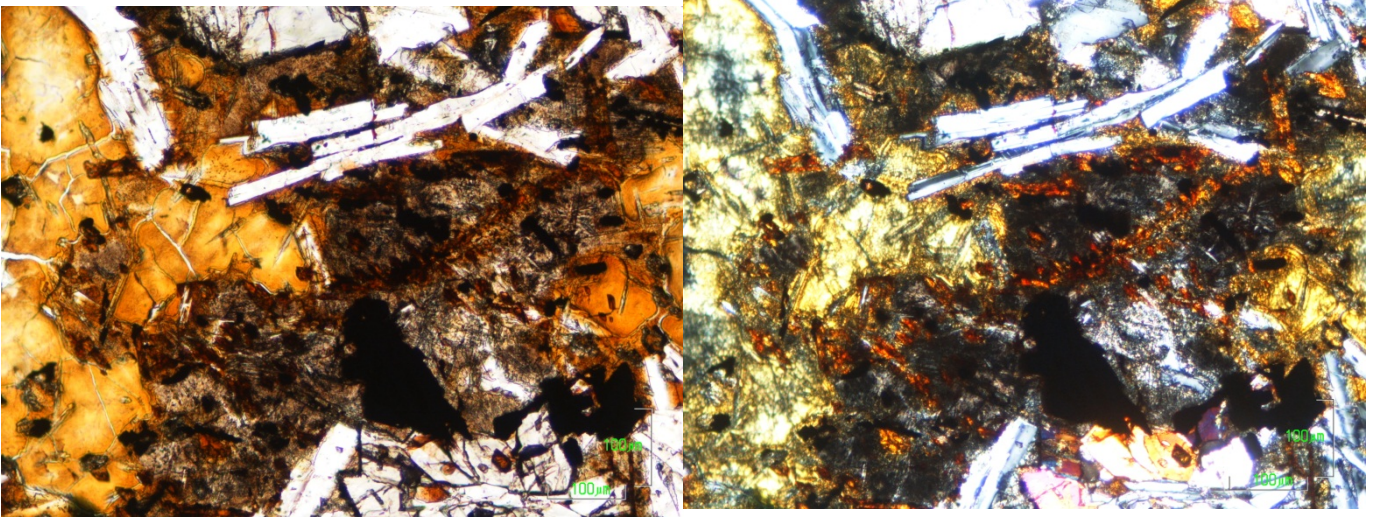
Appendix 13: vesicles and bulk rock (polarized light), sample BT2



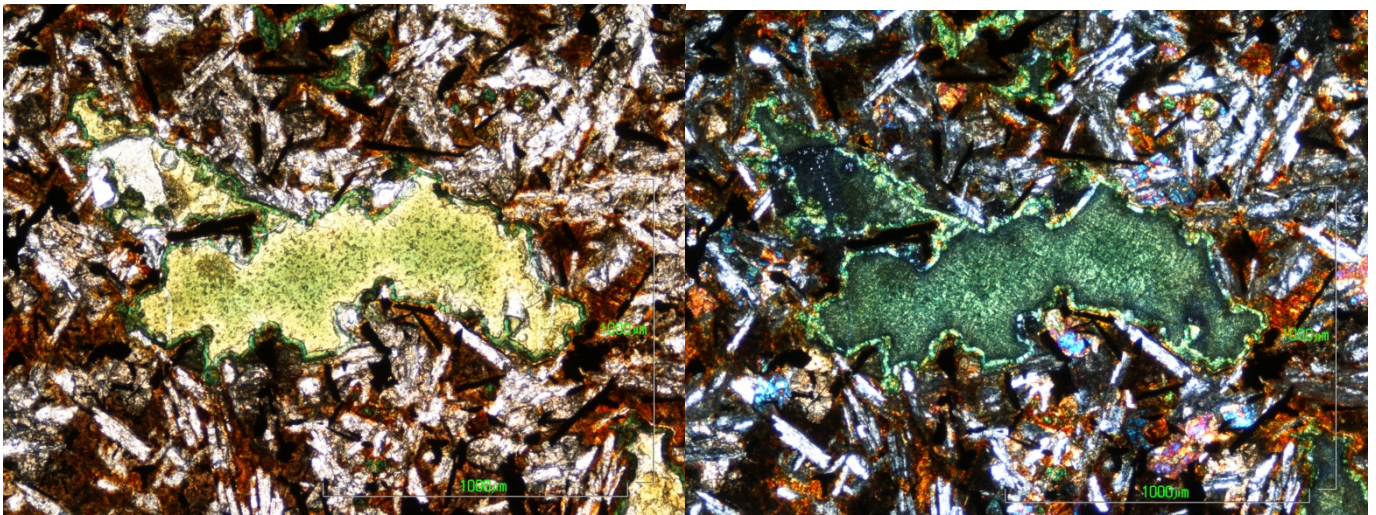
Appendix 14: feldspar with fracturation and oxihydroxides inclusions (natural and polarized light), sample BT2



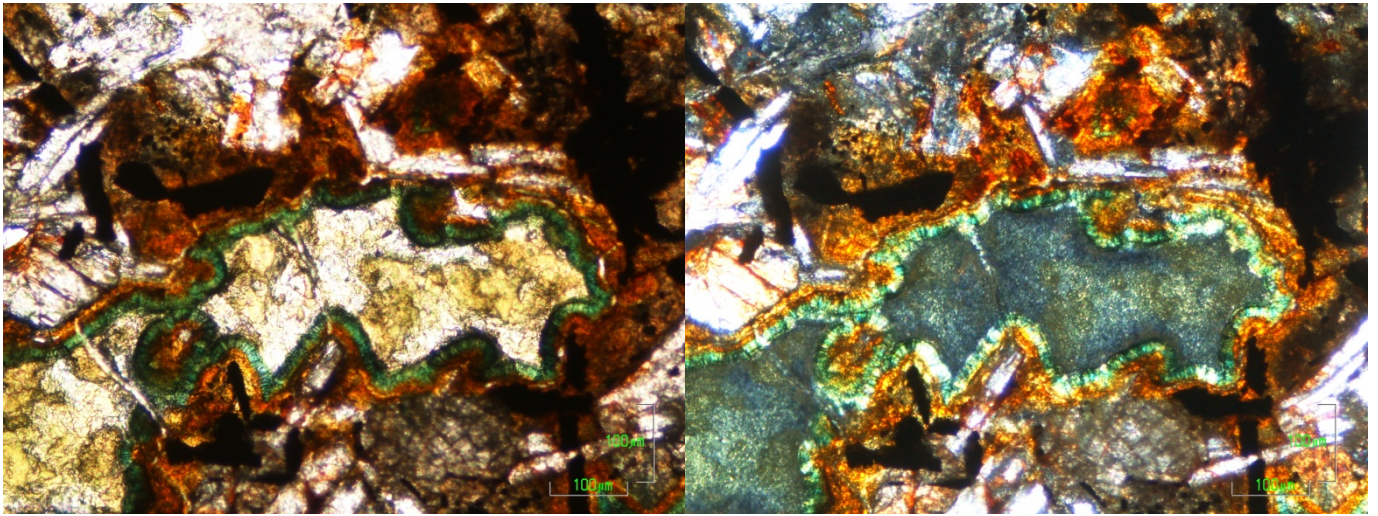
Appendix 15: mesostasis with oxihydroxides inclusions (natural and polarized light), sample BT2



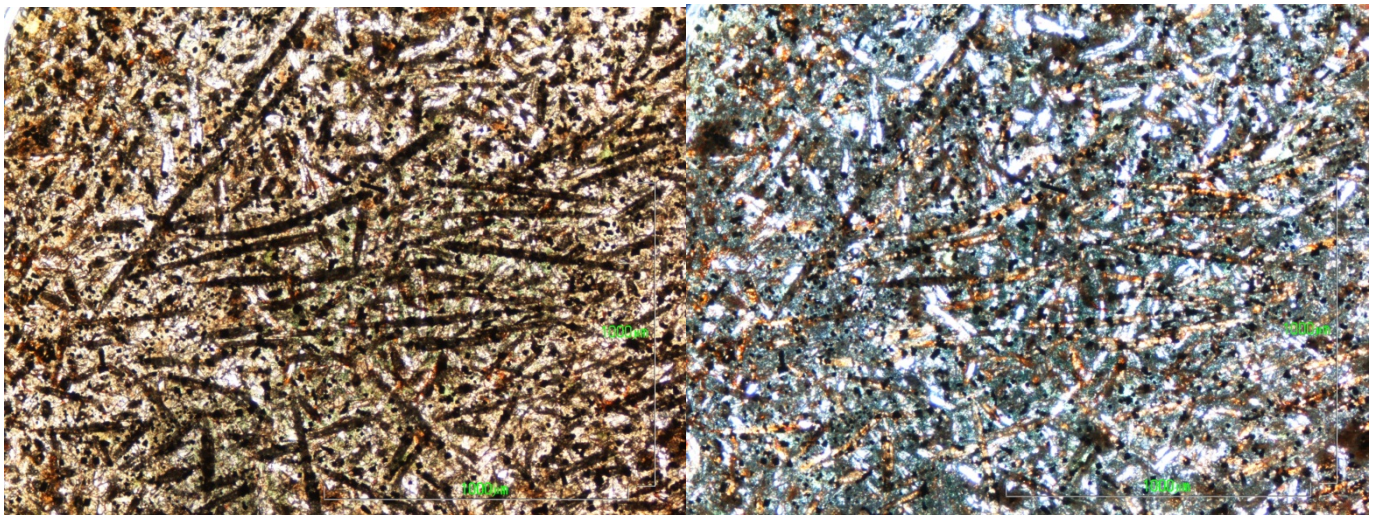
Appendix 16: vesicle filled with green mineral (natural and polarized light), sample BT1A



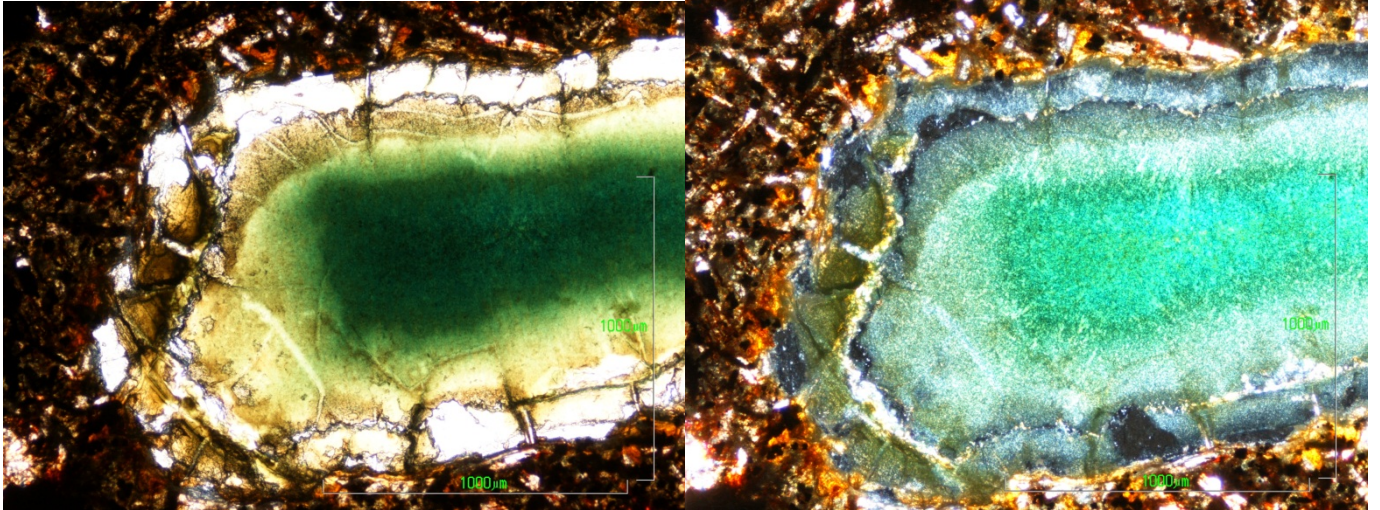
Appendix 17: vesicles with green filling and orange (smectite) alteration around (natural and polarized light), sample BT1A



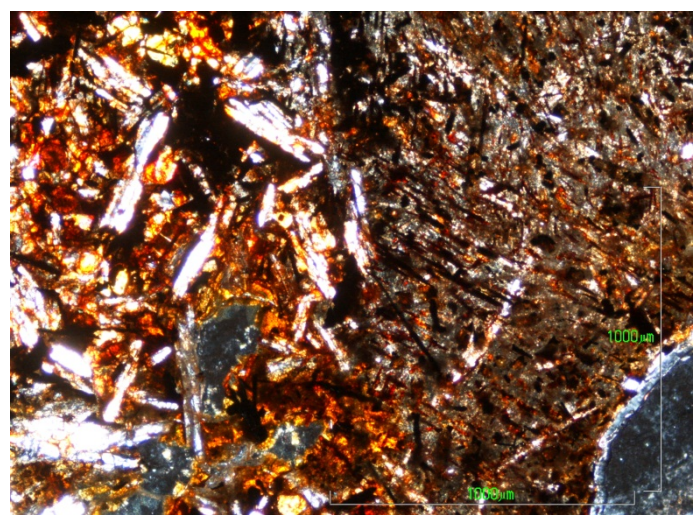
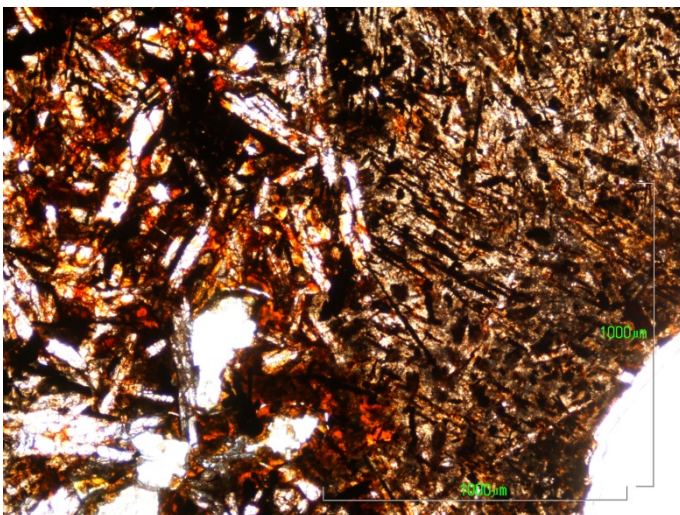
Appendix 18: mesostasis of the special zone (natural and polarized light), sample BT1AA



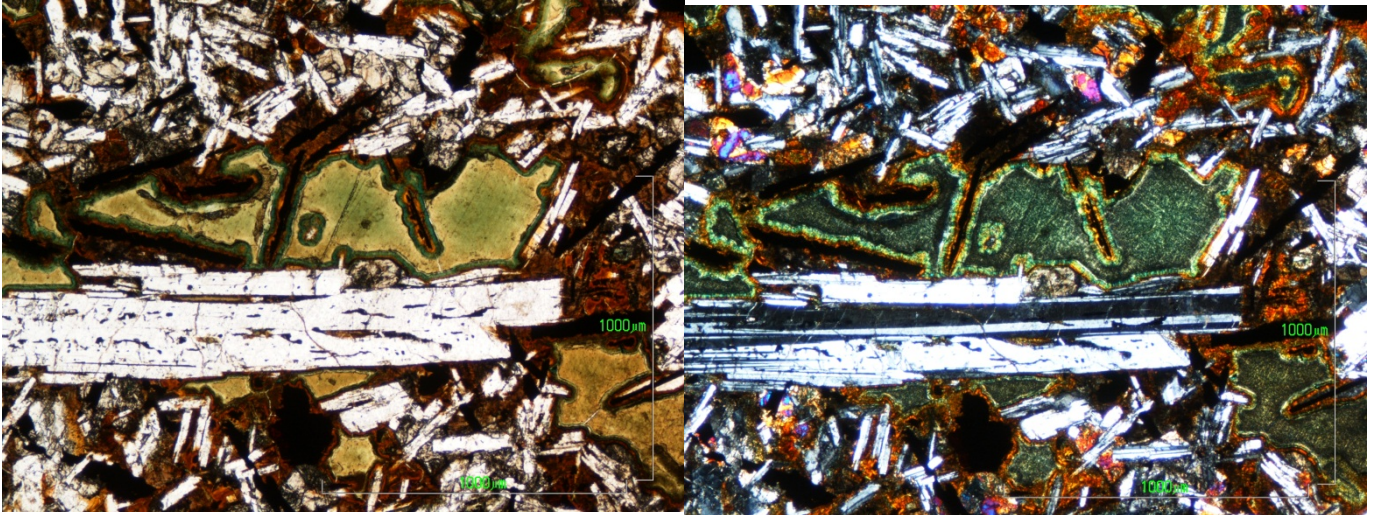
Appendix 19: vesicle of the special zone (natural and polarized light), sample BT1AA



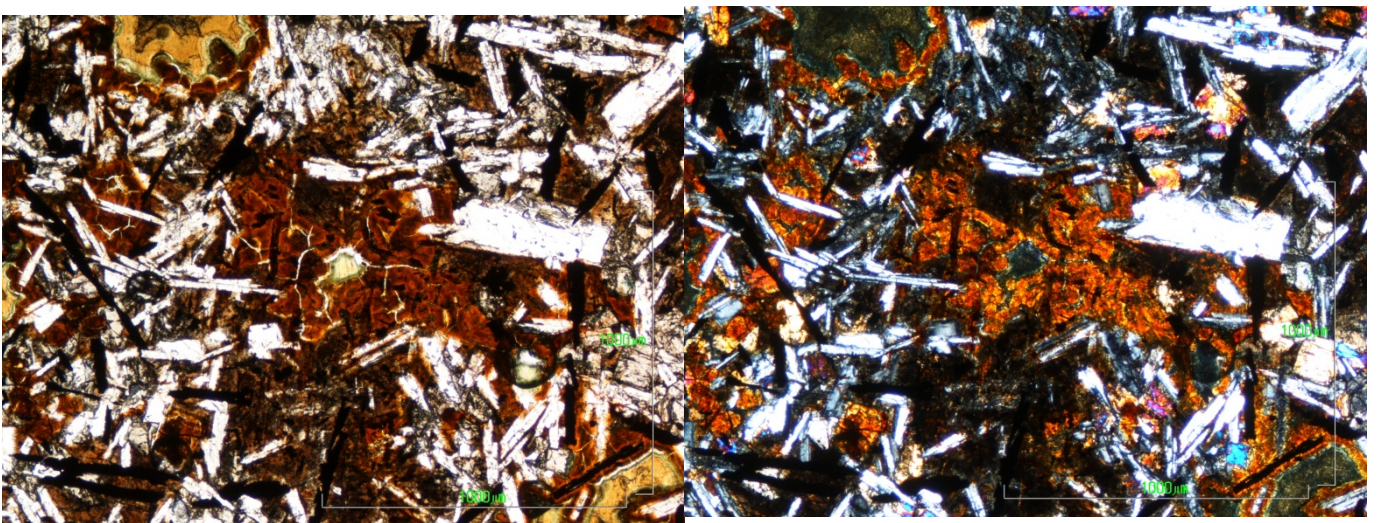
Appendix 20: limit between the special zone and the bulk rock (natural and polarized light), sample BT1AA



Appendix 21: vesicles with an orange layer and two green fillings (natural and polarized light), sample BT1AB

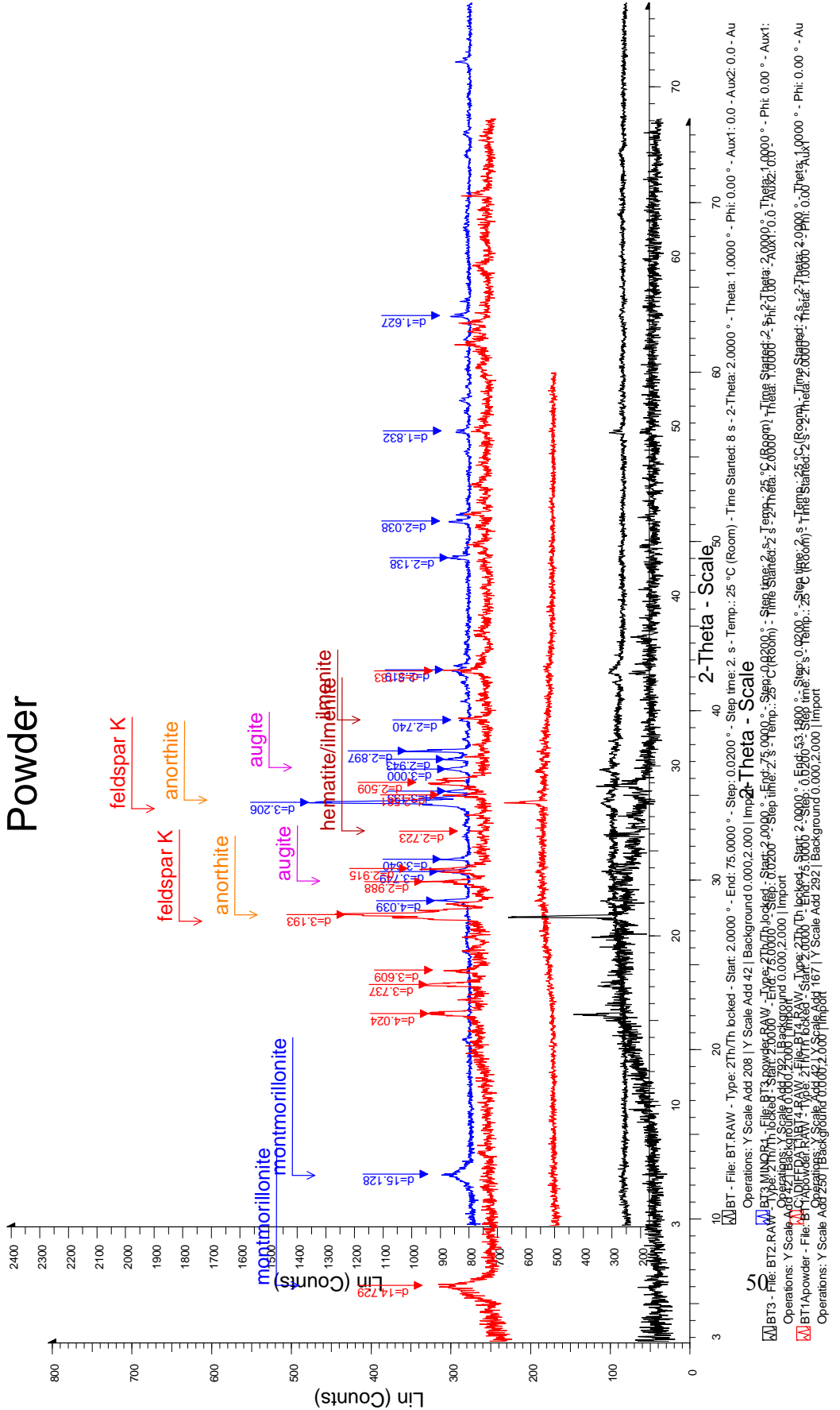


Appendix 22: orange zonation with vesicle in the middle (natural and polarized light), sample BT1AA



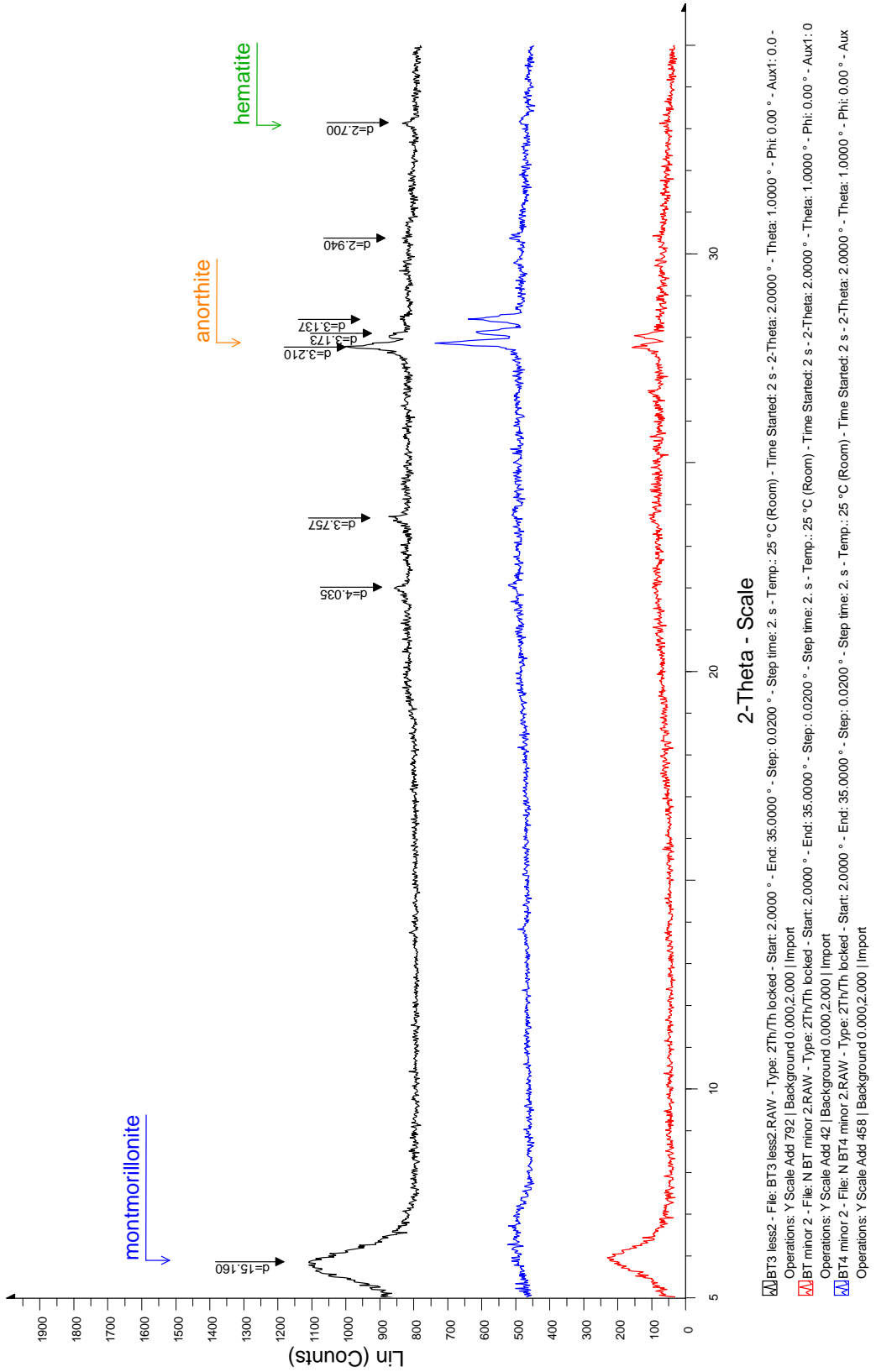
Appendix 23: XRD pattern of powders from different samples

Powder
Powder



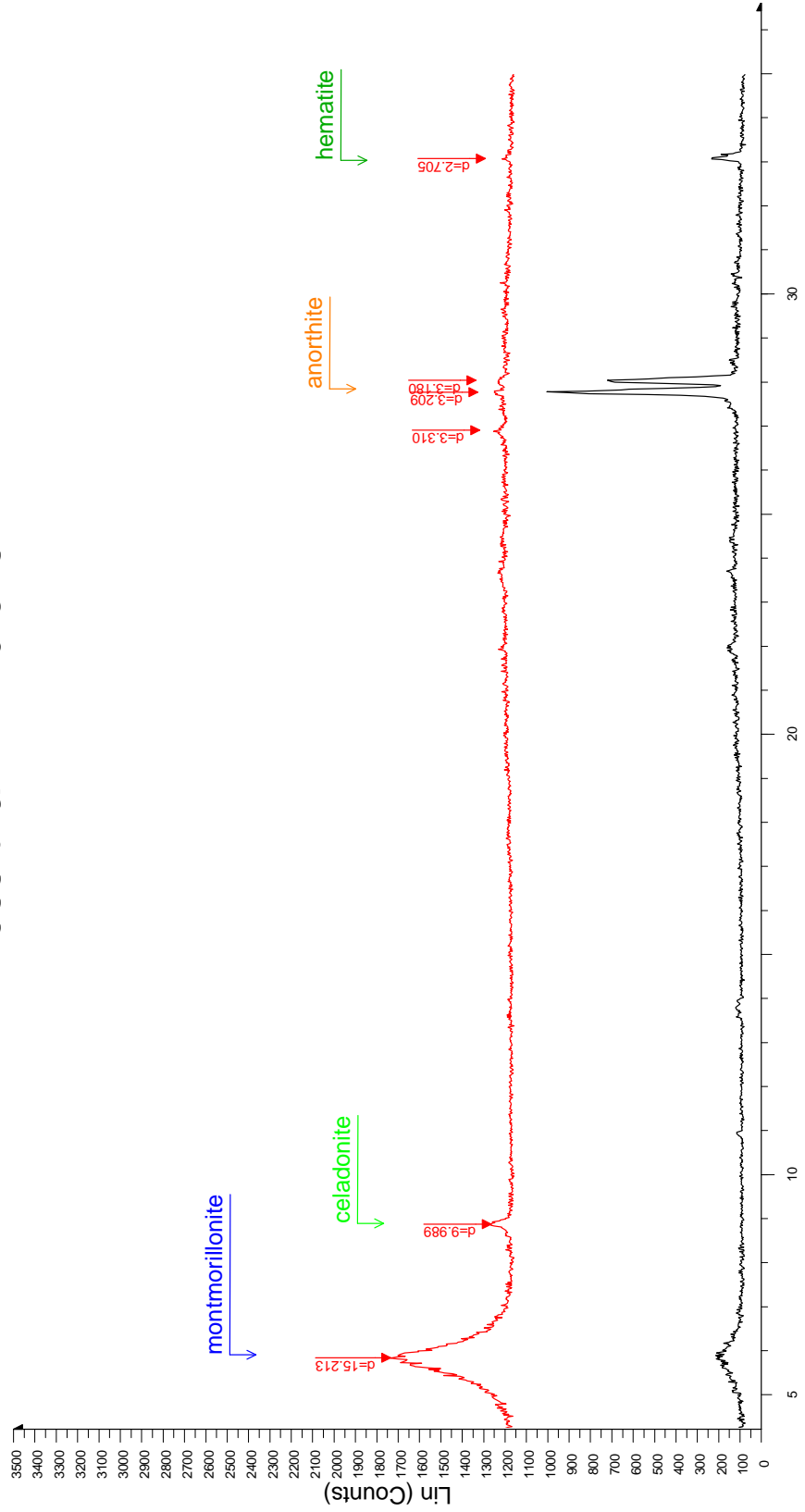
Appendix 24: XRD pattern of oriented slides from different samples

Less than 2 microns



Appendix 25:
XRD pattern of
sample BT3
(powder and
oriented slide)

Less than 2 microns

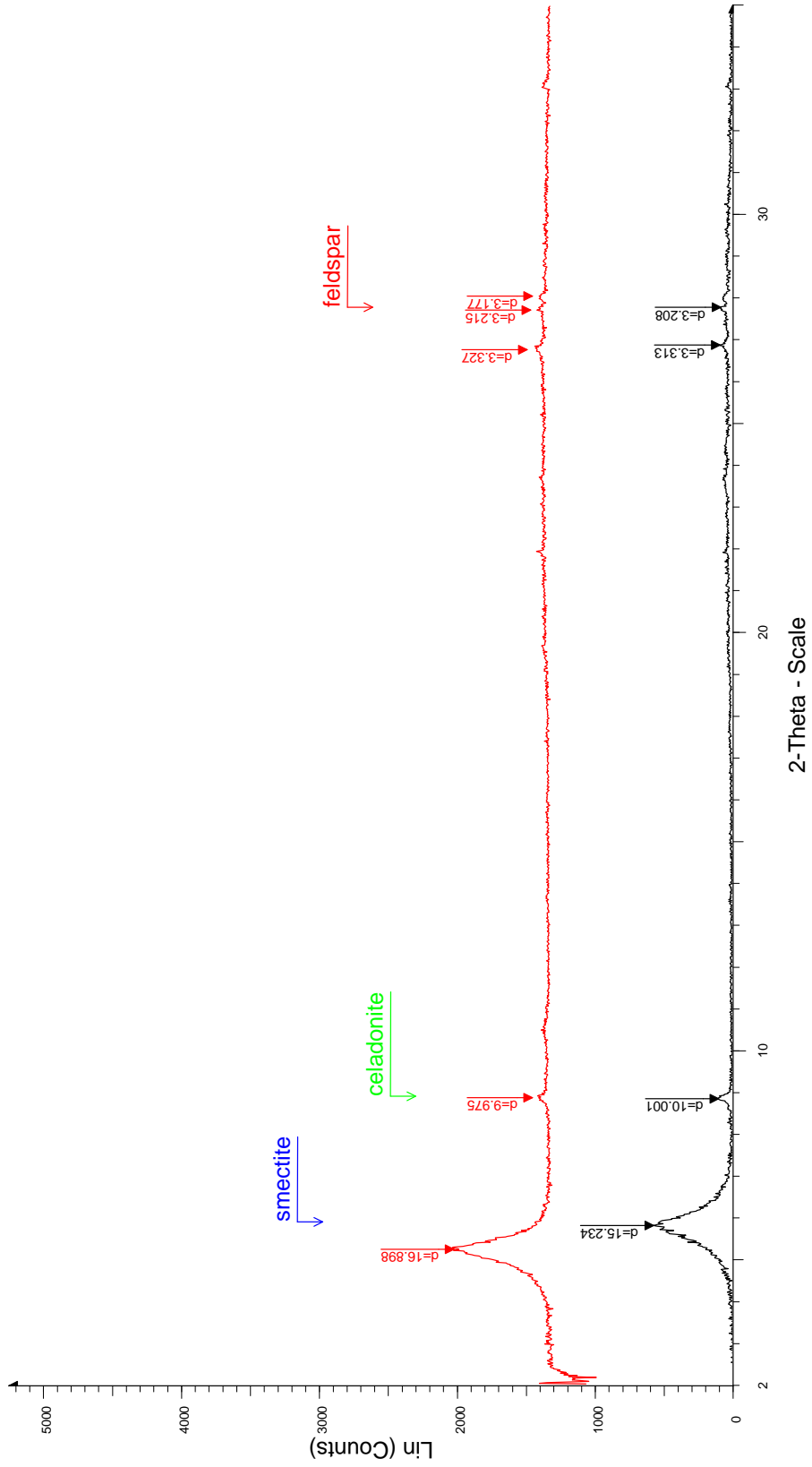


2-Theta - Scale

BT2 minor 2 - File: NBT2 minor 2.RAW - Type: 2Th/Th locked - Start: 2.0000 ° - End: 35.0000 ° - Step: 0.0200 ° - Time Started: 2 s - 2:Theta: 2.0000 ° - Theta: 1.0000 ° - Phi: 0.00 ° - Aux
 Operations: Y Scale Add 83 | Background 0.000,2.000 | Import
 BT1A LESS 2 - File: bt1a LESS 2 ad.RAW - Type: 2Th/Th locked - Start: 2.0000 ° - End: 35.0000 ° - Step: 0.0200 ° - Time Started: 2 s - 2:Theta: 2.0000 ° - Theta: 1.0000 ° - Phi: 0.00 ° - A
 Operations: Y Scale Add 167 | Background 0.000,2.000 | Import

Appendix 26: XRD pattern of sample BT1A (powder and oriented slide)

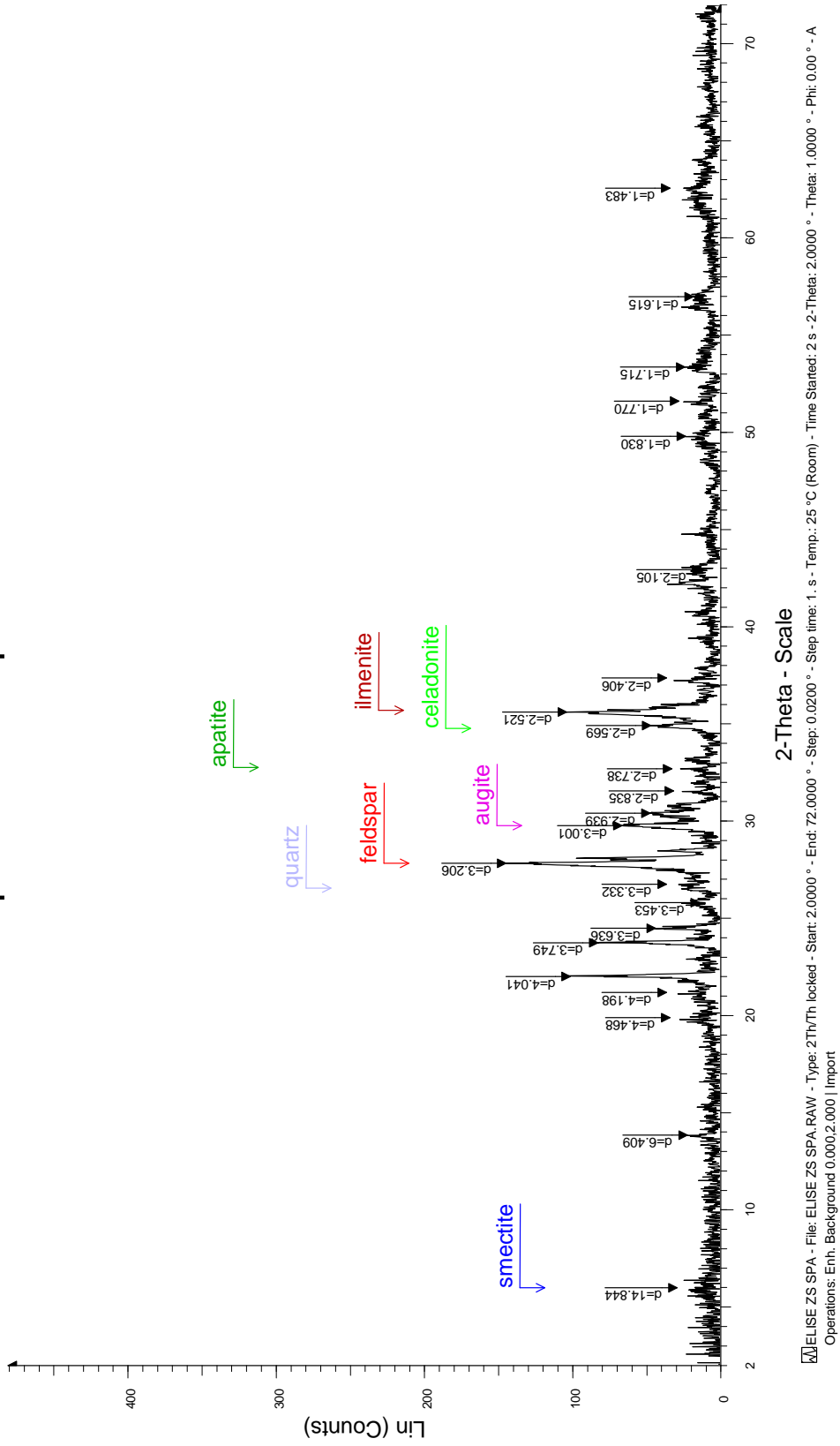
BT1A <2microns AD-EG



BT1A LESS 2 - File: bt1a LESS 2 ad.RAW - Type: 2Th/Th locked - Start: 2.0000 ° - End: 35.0000 ° - Step: 0.0200 ° - Step time: 2. s - Temp.: 25 °C (Room) - Time Started: 2 s - 2-Theta: 2.0000 ° - Theta: 1.0000 ° - Phi: 0.00 ° - A
 Operations: Background 0.000,2.000 | Import
 BT1A in2 EG - File: BT1A in2 EG.RAW - Type: 2Th/Th locked - Start: 2.0000 ° - End: 35.0000 ° - Step: 0.0200 ° - Step time: 2. s - Temp.: 25 °C (Room) - Time Started: 2 s - 2-Theta: 2.0000 ° - Theta: 1.0000 ° - Phi: 0.00 ° - Aux
 Operations: Y Scale Add 333 | Y Scale Add 1000 | Background 0.000,2.000 | Import

Appendix 27: XRD pattern of the powder and oriented slide of the special zone

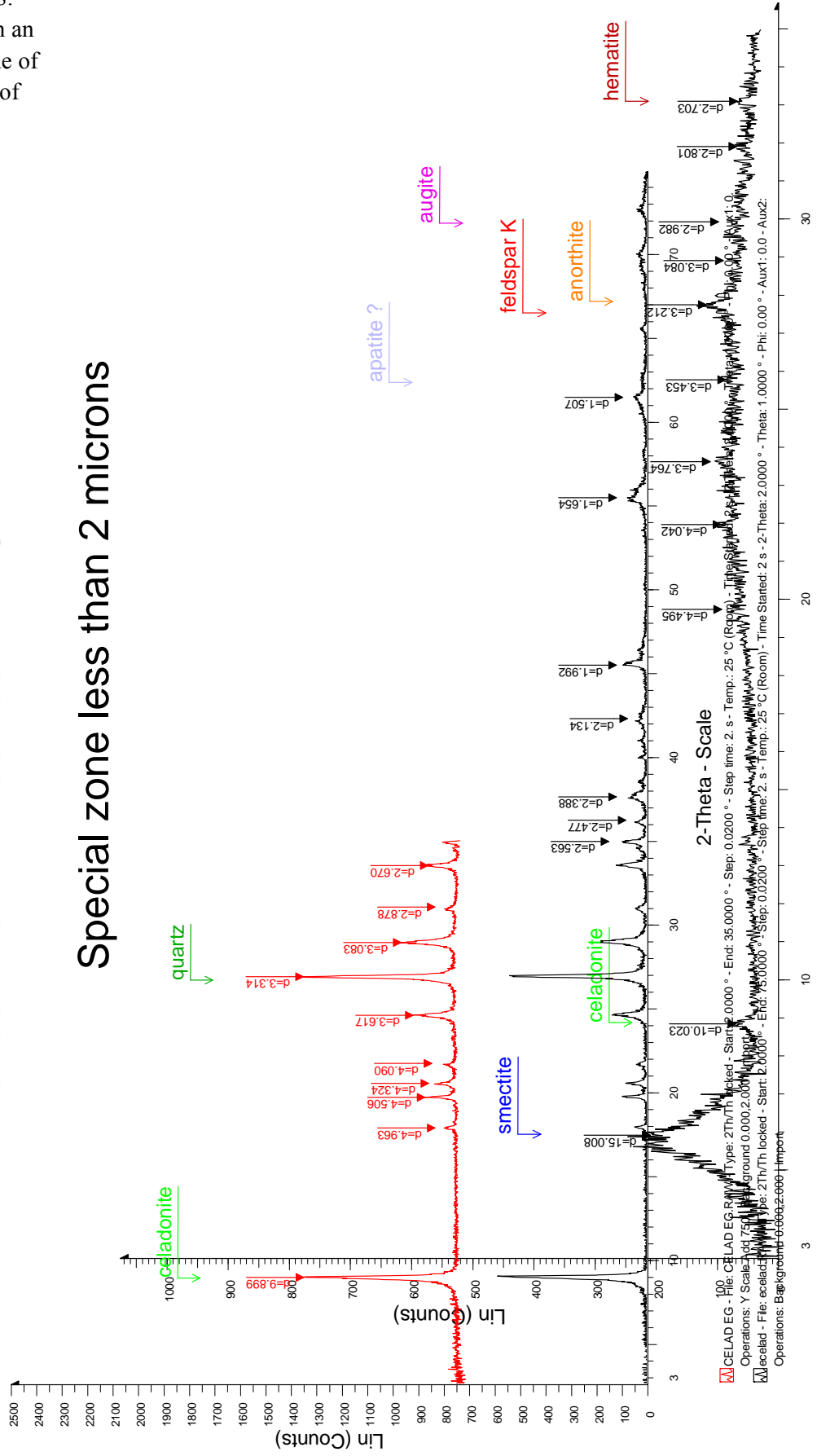
Special zone powder



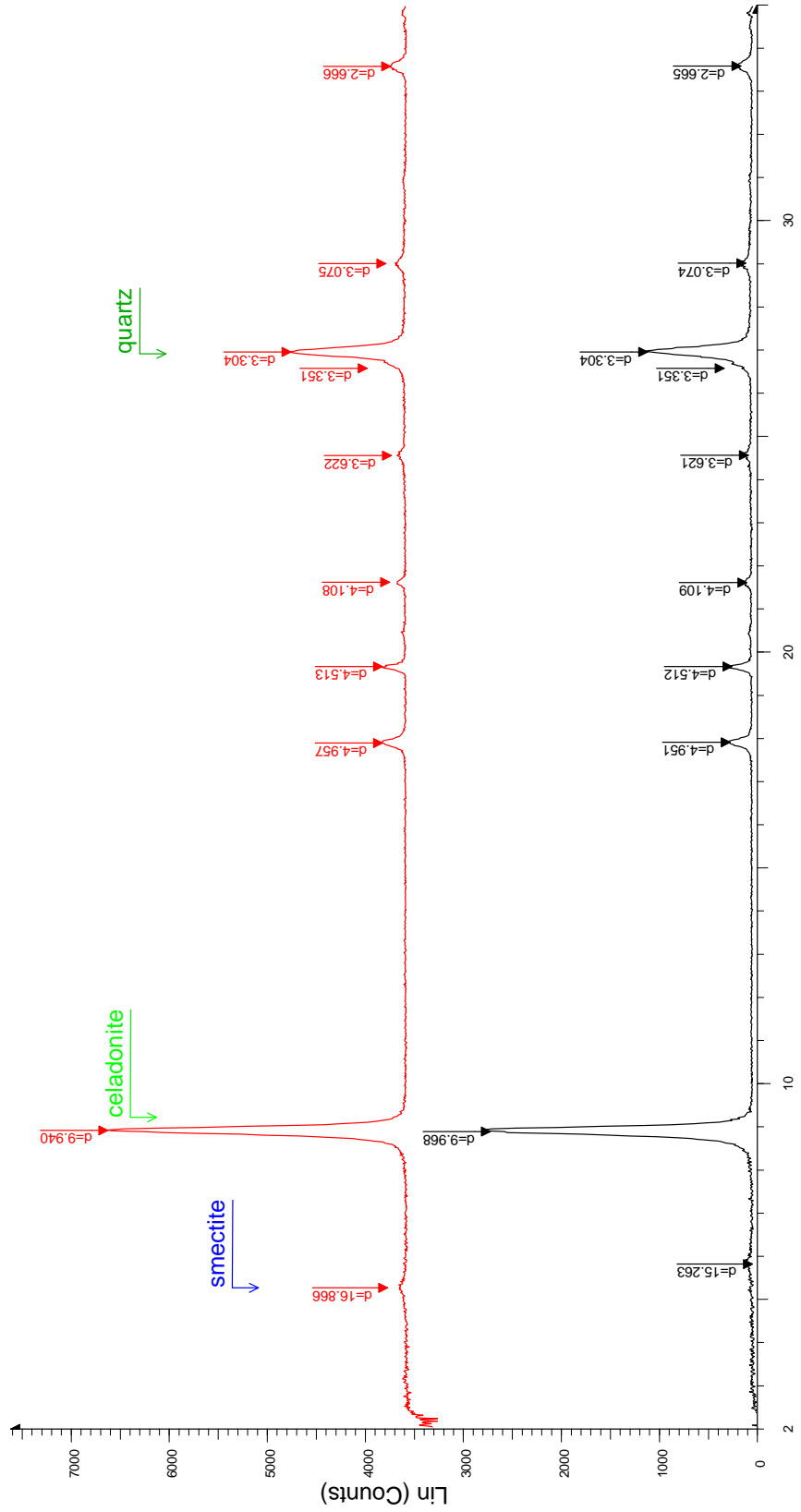
Appendix 28:
XRD pattern an
oriented slide of
the vesicles of
special zone

celadonite from vesicles AD-EG

Special zone less than 2 microns

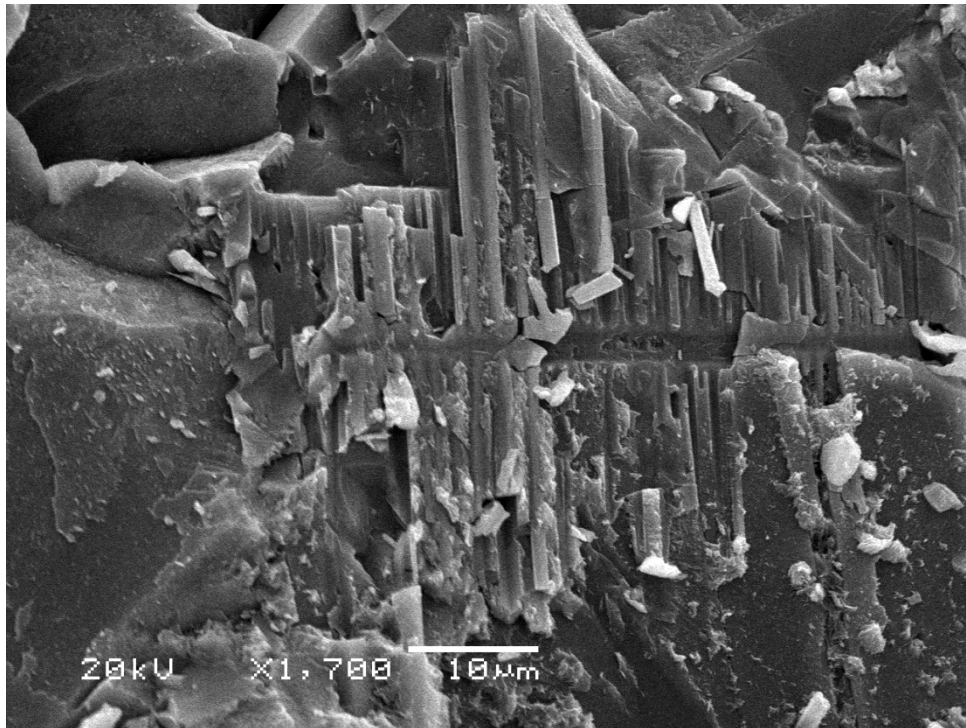


D7 less than 10 micron AD-EG

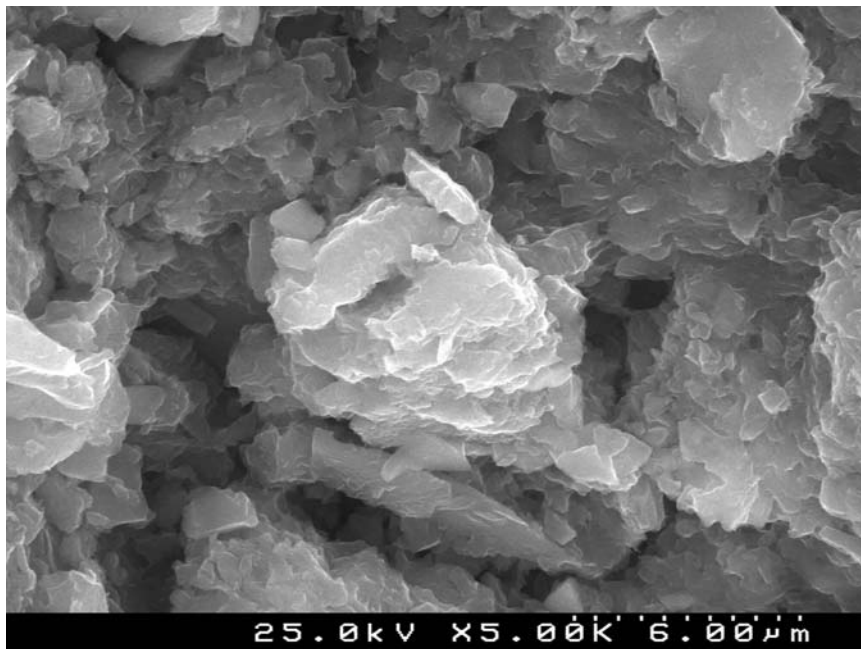


D7 less10 AD - File: D7 less10 AD.RAW - Type: 2Th/Th locked - Start: 2.0000 ° - End: 35.0000 ° - Step: 0.0200 ° - Step time: 2. s - Temp.: 25 °C (Room) - Time Started: 2 s - 2-Theta: 2.0000 ° - Theta: 1.0000 ° - Phi: 0.00 ° - Aux Operations: Y Scale Add 42 | Background 0.000,2.000 | Import
 D7 less10 EG - File: D7 less10 EG.RAW - Type: 2Th/Th locked - Start: 2.0000 ° - End: 35.0000 ° - Step: 0.0200 ° - Step time: 2. s - Temp.: 25 °C (Room) - Time Started: 2 s - 2-Theta: 2.0000 ° - Theta: 1.0000 ° - Phi: 0.00 ° - Aux Operations: Y Scale Add 583 | Y Scale Add 1000 | Background 0.000,2.000 | Import

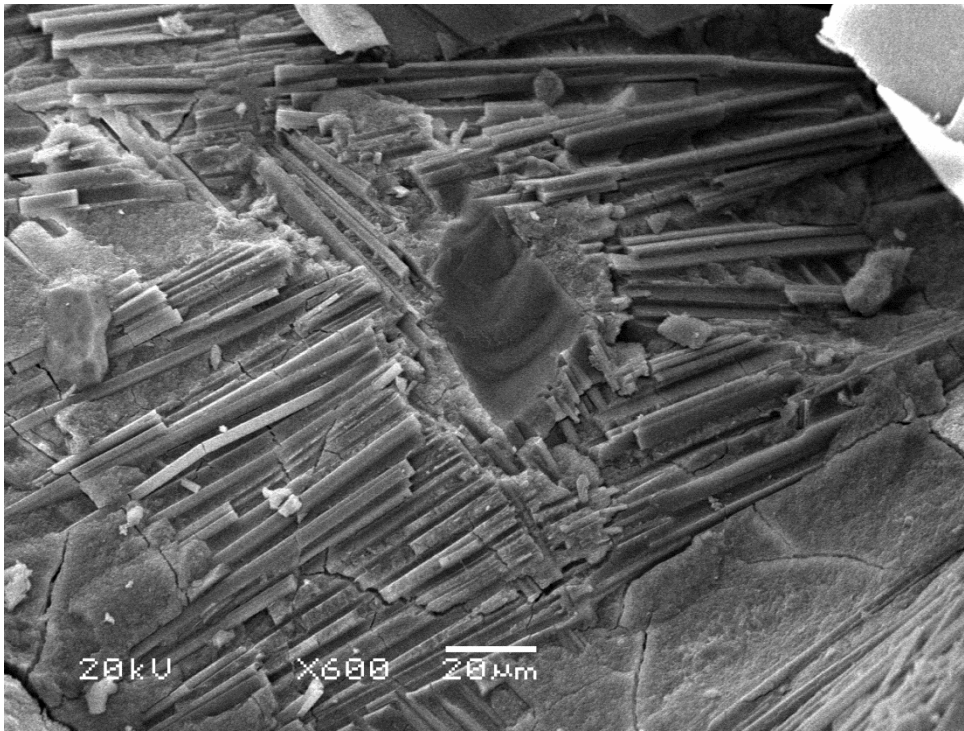
Appendix 30: SEM images of an altered feldspar(plagioclase), BT2



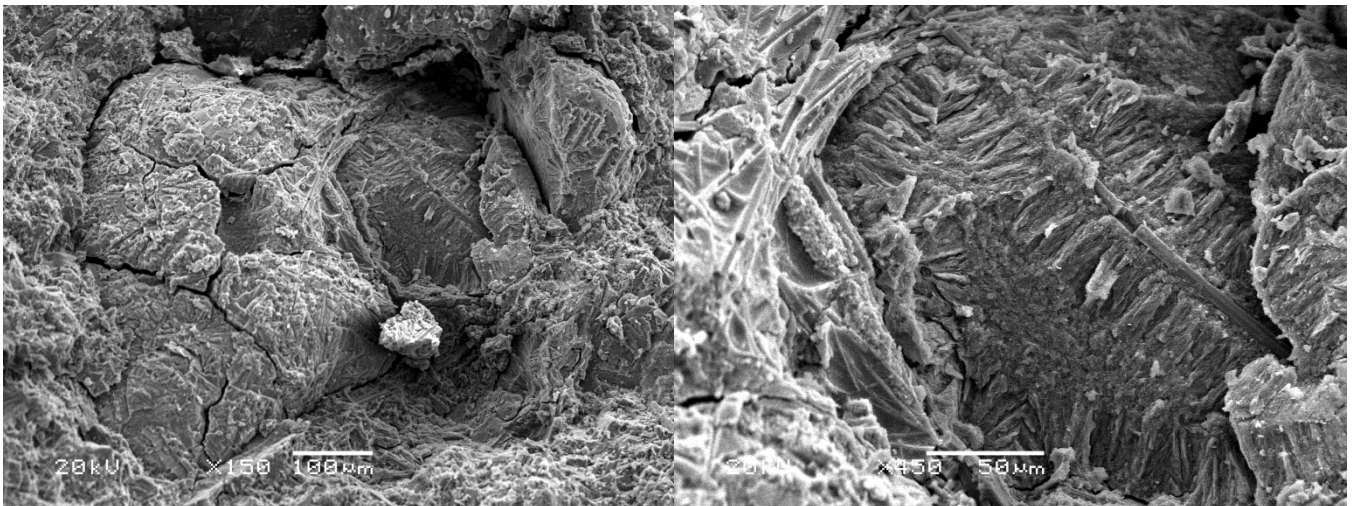
Appendix 31: SEM images of smectite crystallization in the mesostasis, BT4



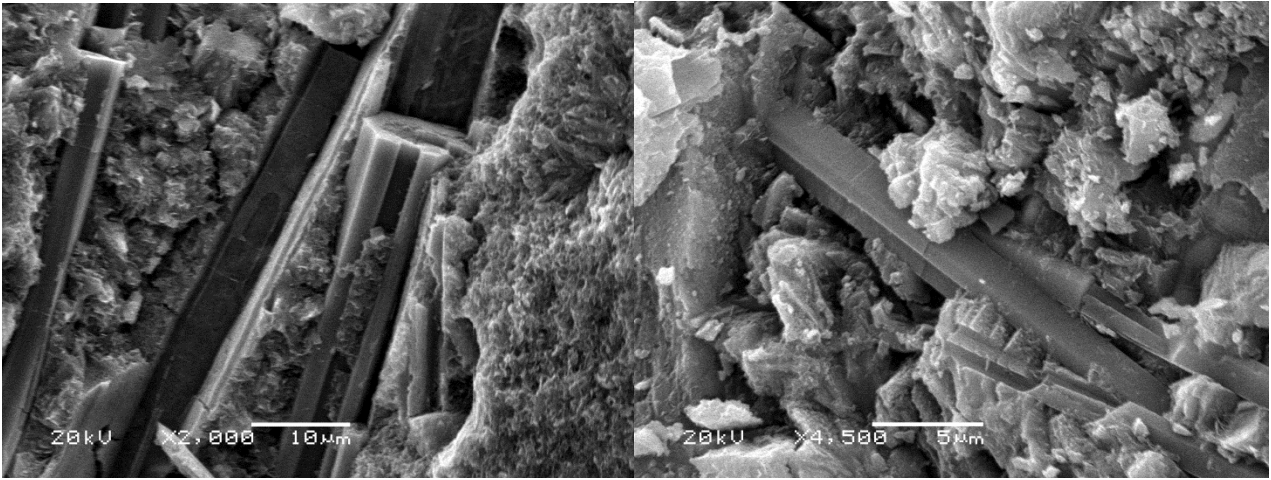
Appendix 31: SEM images of an altered zone with oxides and clay minerals (mesostasis), BT4



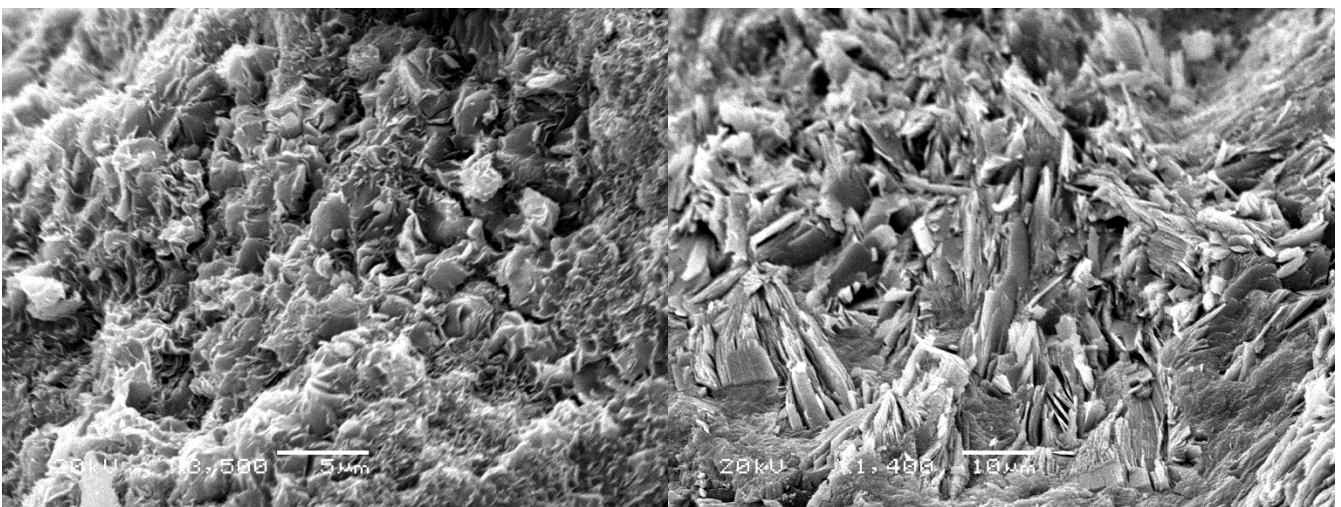
Appendix 32: SEM images of a vesicle in the bulk rock, BT1A



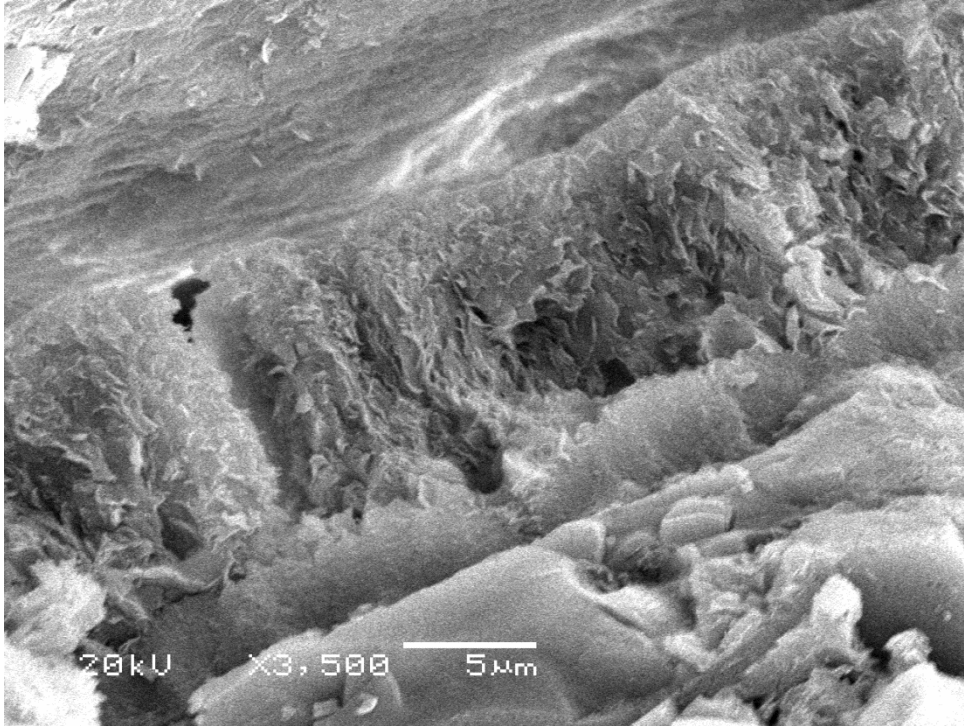
Appendix 33: SEM images of a apatite in the bulk rock, BT1A and BT2



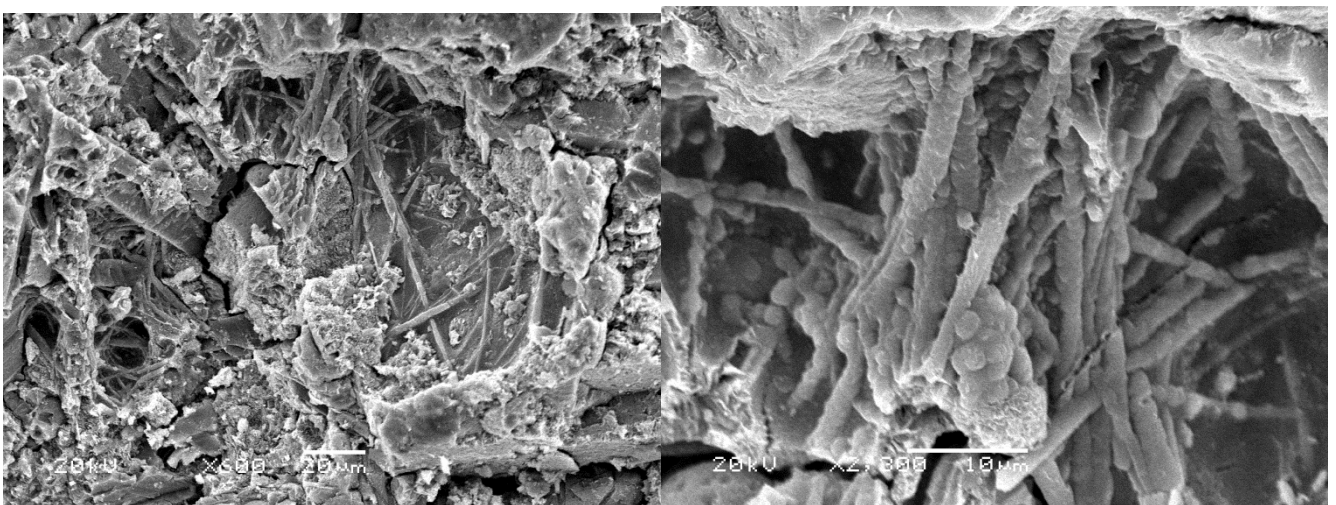
Appendix 34: SEM images of smectite in the mesostasis (left) and celadonite in vesicles (right), special zone



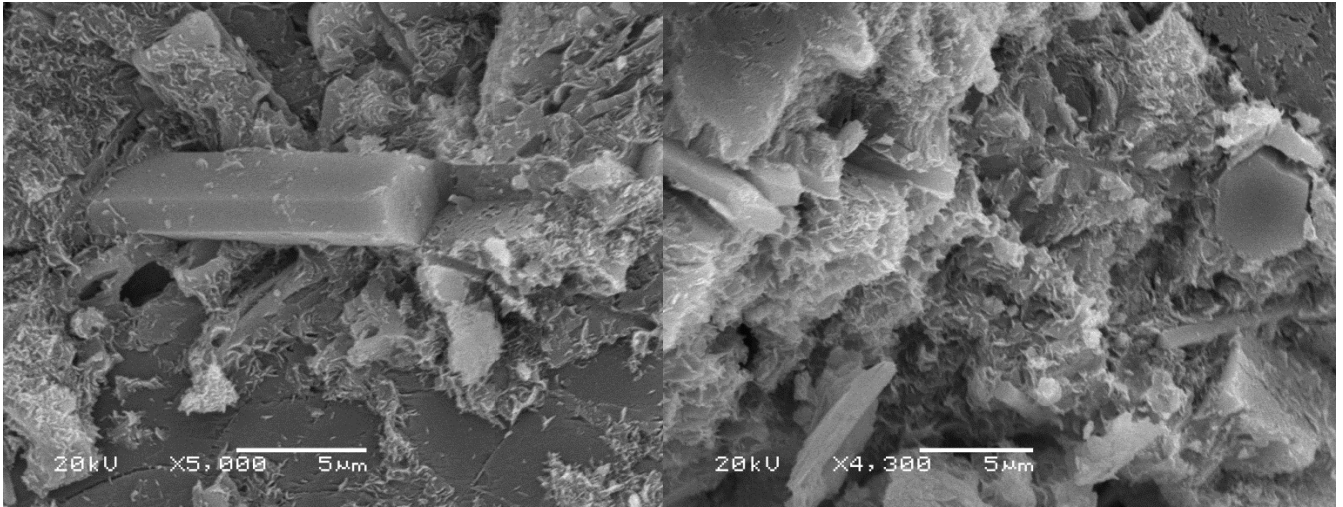
Appendix 35: SEM images of smectite in the border of a big vesicle, special zone



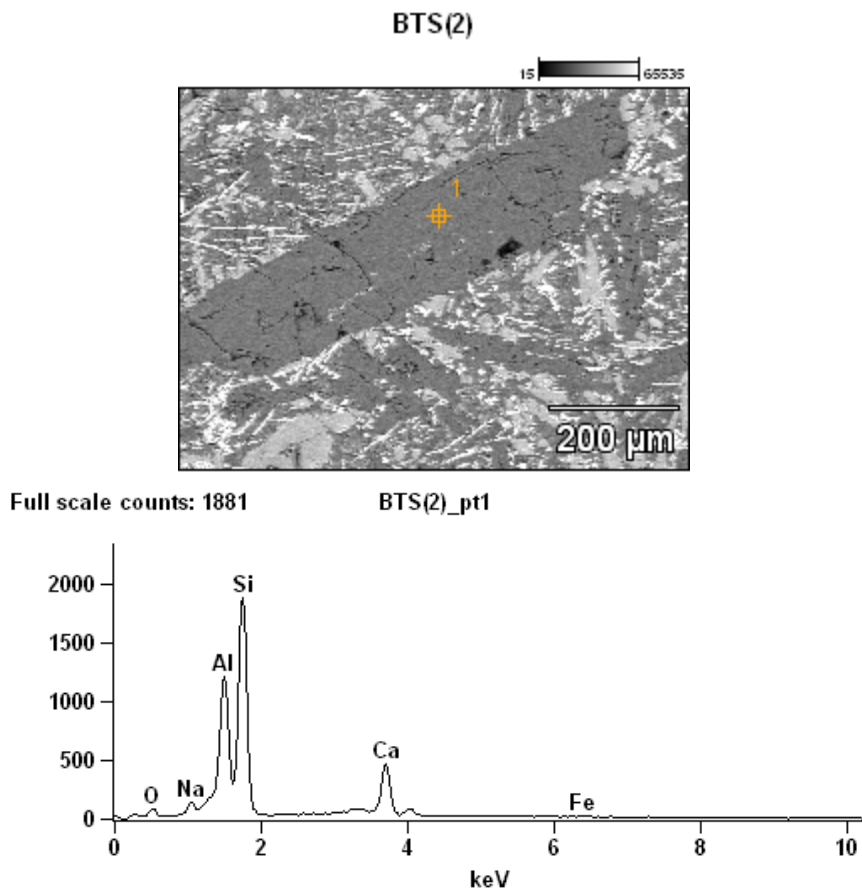
Appendix 36: SEM images of mesostasis in the special zone



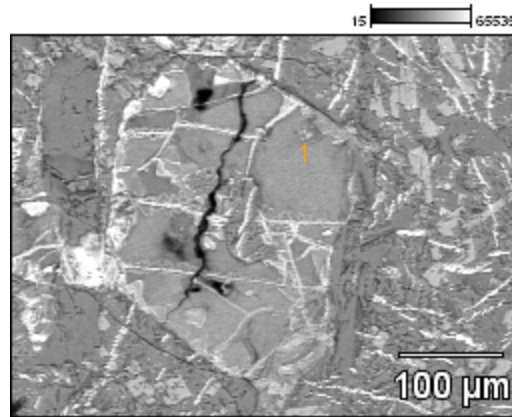
Appendix 37: SEM images of apatite in the special zone



Appendix 38: EDS of macrocrystals of feldspar and pyroxene, BT

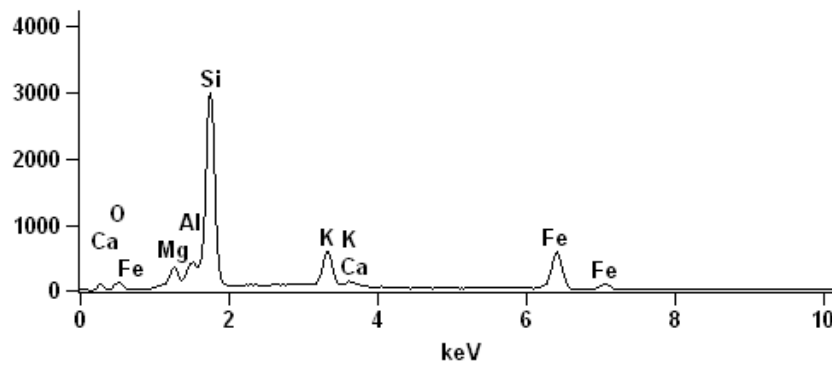


BTS



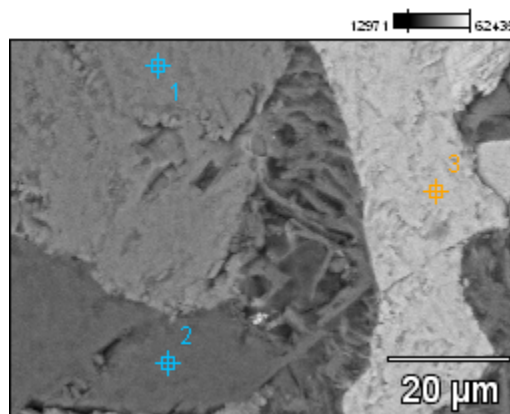
Full scale counts: 2992

BTS_pt1



Appendix 39: EDS of microcrystals of feldspar, pyroxene and titanium oxide, BT4

BT4-7

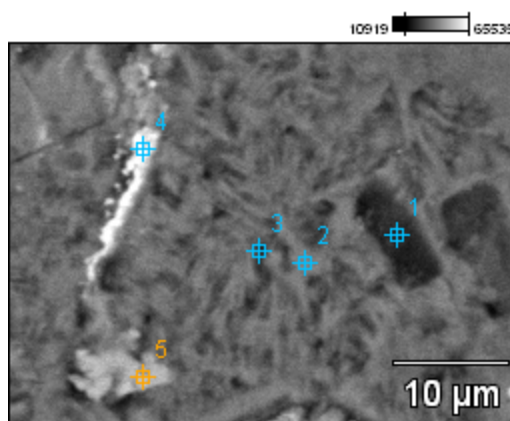


Compound %

	<i>O</i>	<i>Na</i>	<i>Mg</i>	<i>Al</i>	<i>Si</i>	<i>K</i>	<i>Ca</i>	<i>Ti</i>	<i>Fe</i>
<i>BT4-7_pt1</i>	13.40		8.69	1.46	32.91		18.99	1.36	23.19
<i>BT4-7_pt2</i>	16.64	3.69		17.63	45.58	1.28	15.18		
<i>BT4-7_pt3</i>								47.74	52.26

Appendix 40: EDS of mesostasis from BT4 and BT1AA

BT4-14

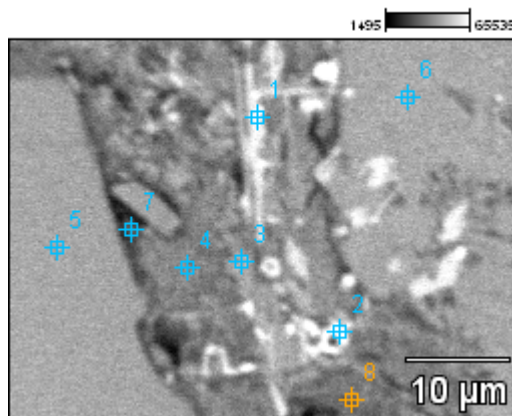


Compound %

	<i>O</i>	<i>Na</i>	<i>Mg</i>	<i>Al</i>	<i>Si</i>	<i>Cl</i>	<i>K</i>	<i>Ca</i>	<i>Ti</i>	<i>Fe</i>
<i>BT4-14_pt1</i>	14.13		5.34	7.99	37.62	4.26	2.89	3.44		24.32
<i>BT4-14_pt2</i>	15.01	1.78		10.83	52.31		15.43	1.50		3.15
<i>BT4-14_pt3</i>			1.24	8.38	57.61		11.57	3.69	1.48	16.03
<i>BT4-14_pt4</i>	6.25		1.30	3.52	13.21		2.66	1.15	0.53	71.37
<i>BT4-14_pt5</i>	12.78		3.98	3.10	28.72		0.51	22.55	1.07	27.29

BT1AA 11

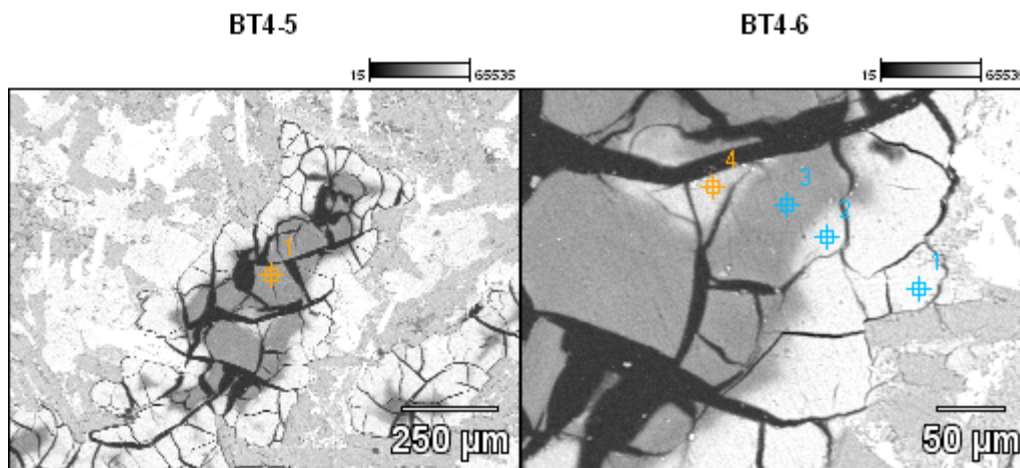
Compound %



	<i>O</i>	<i>Na</i>	<i>Mg</i>	<i>Al</i>	<i>Si</i>	<i>P</i>	<i>K</i>	<i>Ca</i>	<i>Ti</i>	<i>Fe</i>
--	----------	-----------	-----------	-----------	-----------	----------	----------	-----------	-----------	-----------

BT1AA									
11_pt1	11.05		0.57	3.20	15.44	0.16	37.52		32.05
BT1AA									
11_pt2	7.46		0.51	1.73				0.95	89.35
BT1AA									
11_pt3	19.24	1.68	10.22	52.72		16.14			
BT1AA									
11_pt4	18.22		3.07	6.29	42.89		2.50	3.04	3.12
BT1AA									
11_pt5	19.77	4.39		18.25	43.12		1.31	13.16	
BT1AA									
11_pt6	20.62	1.86		9.52	53.94		14.05		
BT1AA									
11_pt7	11.05		1.49	17.86	29.19			40.41	
BT1AA									
11_pt8	12.04		3.00	6.27	38.17		3.09	3.55	7.68

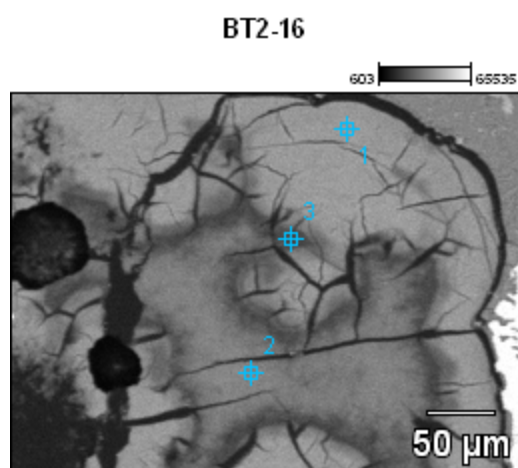
Appendix 41: first type of vesicles in BT4



Compound %

	<i>O</i>	<i>Mg</i>	<i>Al</i>	<i>Si</i>	<i>Ca</i>	<i>Fe</i>
BT4-6_pt1	13.48	8.15	5.66	31.58	4.73	36.40
BT4-6_pt2	13.25	7.23	4.83	34.33	5.02	35.35
BT4-6_pt3	12.44	6.99	5.27	35.89	4.84	34.57
BT4-6_pt4	11.77	7.85	4.20	35.40	4.37	36.42

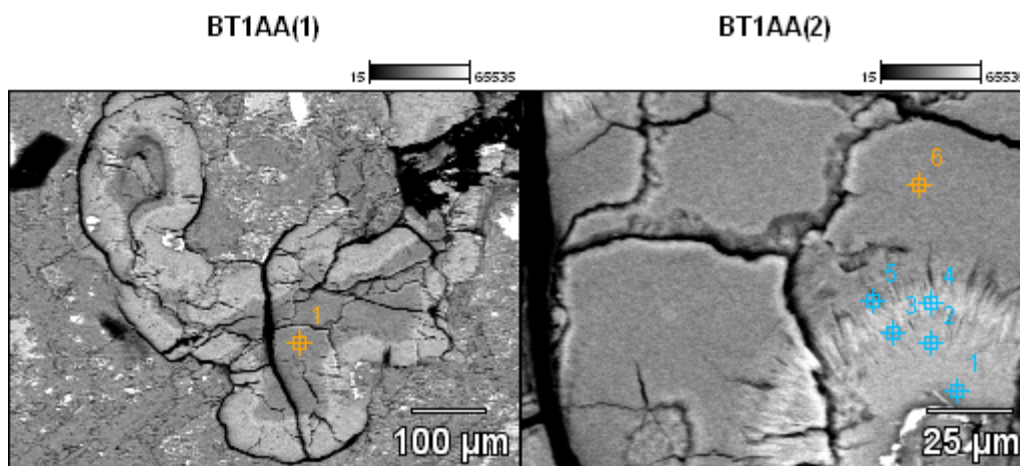
Appendix 42: first type of vesicles in BT2



Compound %

	<i>O</i>	<i>Mg</i>	<i>Al</i>	<i>Si</i>	<i>K</i>	<i>Ca</i>	<i>Fe</i>
<i>BT2-16_pt1</i>	11.94	7.74	6.63	32.68		4.31	36.70
<i>BT2-16_pt2</i>	13.32	5.08	4.97	42.50	1.16	2.39	30.57
<i>BT2-16_pt3</i>	15.16	3.34	3.72	39.77	1.30	3.24	33.48

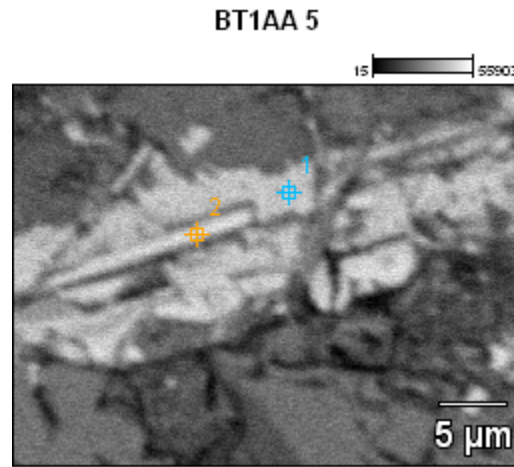
Appendix 43: EDS analysis of second type of vesicles in BT1AA



Compound %

	<i>O</i>	<i>Mg</i>	<i>Al</i>	<i>Si</i>	<i>K</i>	<i>Ca</i>	<i>Fe</i>
<i>BT1AA(2)_pt1</i>	18.49	6.30	7.56	32.57	0.33	4.24	30.51
<i>BT1AA(2)_pt2</i>	16.72	6.53	7.59	32.96	0.29	4.20	31.72
<i>BT1AA(2)_pt3</i>	15.85	4.79	7.59	34.92	4.61	2.28	29.96
<i>BT1AA(2)_pt4</i>	17.16	2.34	6.36	35.40	11.44	0.68	26.62
<i>BT1AA(2)_pt5</i>	16.74	4.89	7.97	36.12	1.93	3.33	29.02
<i>BT1AA(2)_pt6</i>	13.88	1.75	7.45	42.21	2.55	3.15	29.01

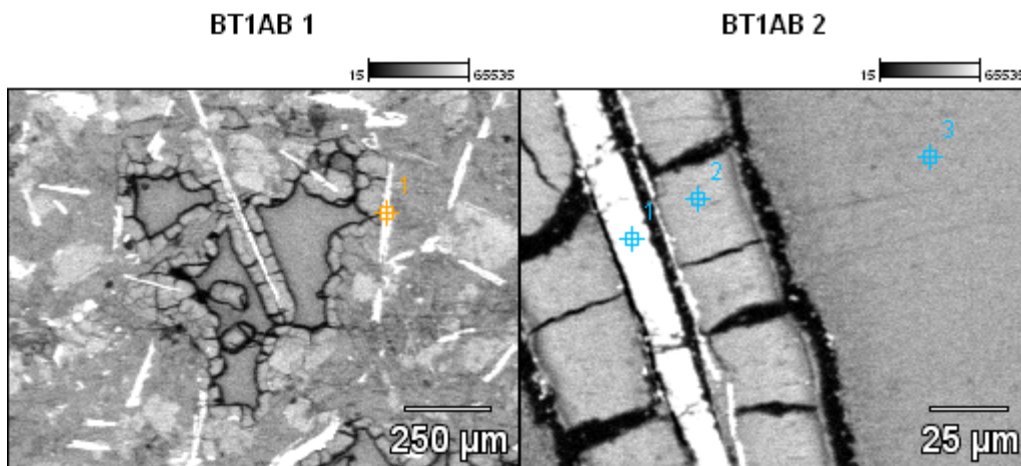
Appendix 44: EDS analysis of hydroxyapatite in BT1AA



Compound %

	<i>O</i>	<i>Mg</i>	<i>Al</i>	<i>Si</i>	<i>P</i>	<i>K</i>	<i>Ca</i>	<i>Fe</i>
<i>BT1AA 5_pt1</i>	15.14	6.41		31.72			11.34	35.39
<i>BT1AA 5_pt2</i>	9.32		0.58	2.55	24.69	0.94	61.91	

Appendix 45: EDS analysis of second type of vesicles in BT1AB

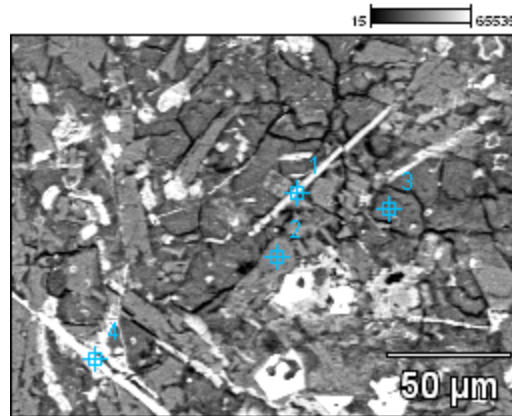


Compound %

	<i>O</i>	<i>Mg</i>	<i>Al</i>	<i>Si</i>	<i>K</i>	<i>Ca</i>	<i>Ti</i>	<i>Fe</i>
<i>BT1AB 2_pt1</i>	11.33			0.46			47.29	40.92
<i>BT1AB 2_pt2</i>	19.31	7.54	5.12	32.98		6.03		29.02
<i>BT1AB 2_pt3</i>	14.19	3.62	4.21	40.40	4.53	3.43		29.62

Appendix 46: EDS analysis of special zone in BT1AA

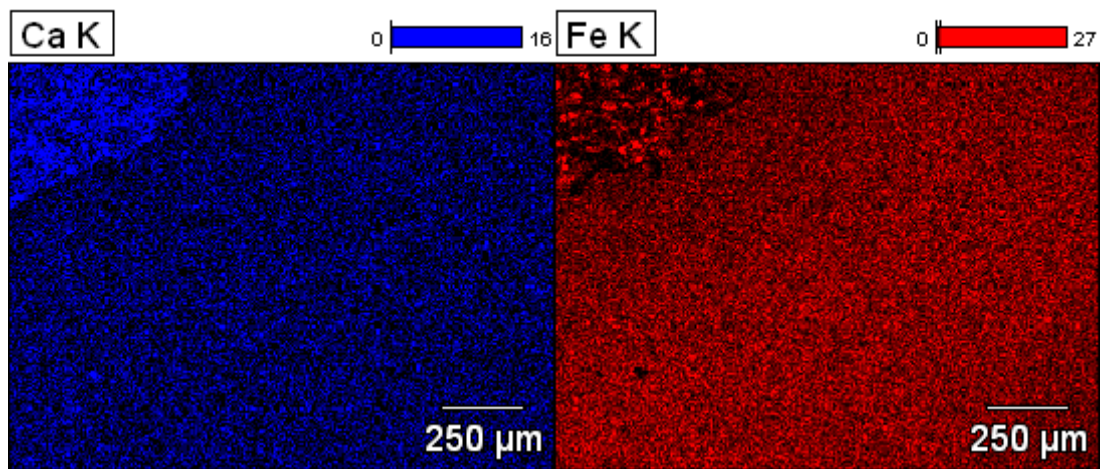
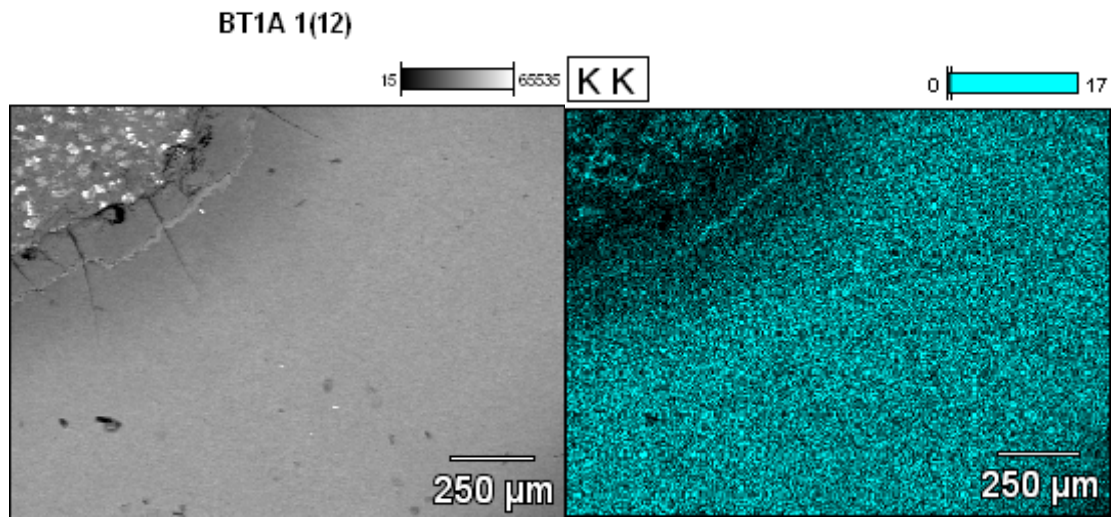
BT1AA(7)



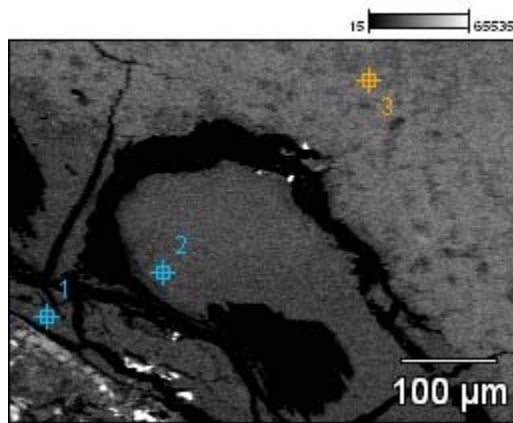
Compound %

	<i>O</i>	<i>Na</i>	<i>Mg</i>	<i>Al</i>	<i>Si</i>	<i>P</i>	<i>K</i>	<i>Ca</i>	<i>Ti</i>	<i>Fe</i>
<i>BT1AA(7)_p</i>										
<i>t1</i>				0.57	3.97	26.31		69.15		
<i>BT1AA(7)_p</i>										
<i>t2</i>	21.04	2.93		18.54	45.03		1.52	10.94		
<i>BT1AA(7)_p</i>										
<i>t3</i>	12.24		2.41	11.89	48.32		1.32	2.66		21.16
<i>BT1AA(7)_p</i>										
<i>t4</i>	7.23		0.48	0.76	2.49			0.43	35.97	52.63

Appendix 47: EDS analysis of vesicles of special zone in BT1AA



BT1AA 3

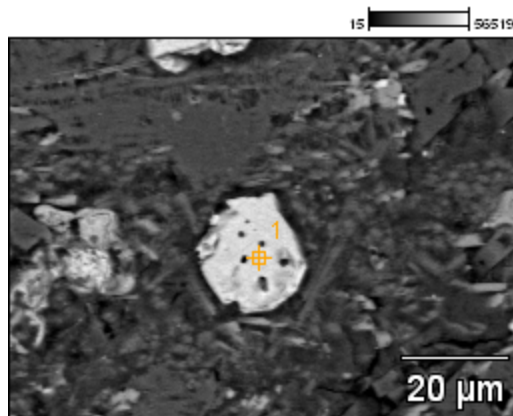


Compound %

	<i>O</i>	<i>Mg</i>	<i>Al</i>	<i>Si</i>	<i>K</i>	<i>Ca</i>	<i>Fe</i>
BT1AA 3_pt1	18.71	2.75	6.10	38.91	3.00	8.49	22.04
BT1AA 3_pt2	16.94	3.10	5.73	41.17	5.16	2.35	25.55
BT1AA 3_pt3	16.84	3.44	3.53	36.74	13.68		25.77

Appendix 48: EDS analysis of two types of oxides in special zone and normal zone, BT1A

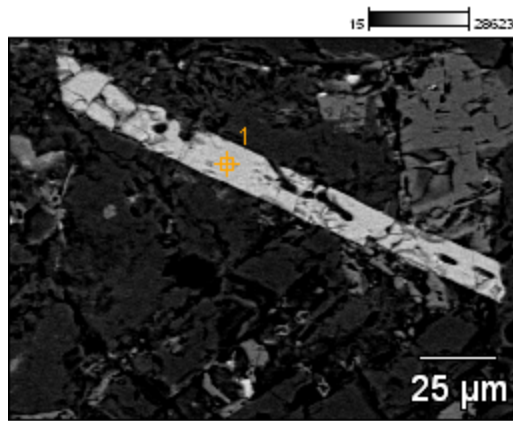
BT1A 1(2)



Compound %

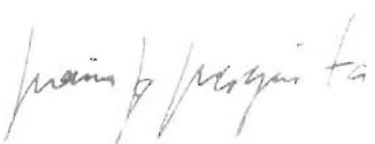
	<i>O</i>	<i>Al</i>	<i>Ti</i>	<i>Fe</i>
BT1A 1(2)_pt1	5.35	1.21	15.90	77.54

BT1A 1(3)



Compound %

	<i>O</i>	<i>Ti</i>	<i>Fe</i>
BT1A 1(3)_pt1	7.62	42.94	49.44

ANEXO I	
Título da Dissertação:	
<p>Título: Estudo das Argilas das Rochas Basálticas da Formação Serra Geral no Rio Grande do Sul. Argilominerais em lavas portadoras de ametista na região do Alto Uruguai (RS), Província Magmática do Paraná.</p>	
Área de Concentração: GEOQUÍMICA	
Autor: Elise Mulocher	
Orientador: André Sampaio Mexias	
Examinador: Maria José Mesquita	
Data: 28 de abril de 2013	
Conceito: A	
PARECER:	
<p>A dissertação tem um objetivo claro a desenvolver, "estudar e entender como se formaram os argilominerais presentes no derrame 6, mineralizado a ametista". Diversas técnicas analíticas em amostras coletadas em um pequeno perfil da rocha encaixante basáltica até o geodo mineralizado foram realizadas. As técnicas empregadas envolvem análises como difração de raio X, SEM, BSE, EDS para estudar morfologia e composição química dos minerais que compõem a rocha, bem como dos argilominerais nos diferentes ambientes.</p> <p>Os resultados são plenamente condizentes com uma dissertação de mestrado, muitos dados foram coletados e técnicas bem desenvolvidas. Sugere-se um aprofundamento nas discussões. As hipóteses são levantadas, mas pouco desenvolvidas. Sugiro igualmente um cuidado com o resumo e com a colocação de parte das figuras em anexo para o texto principal.</p>	
	
Assinatura:	Data: 28/04/2013
Ciente do Orientador:	
Ciente do Aluno:	

ANEXO I

Título da Dissertação/Tese:

Estudo das Argilas das Rochas Basálticas da Formação Serra Geral no Rio Grande do Sul. Argilominerais em lavas portadoras de ametista na região do Alto Uruguai (RS), Província Magmática do Paraná.

Área de Concentração: **Geoquímica**

Autora: **Elise Mulocher**

Orientador: Prof. Dr. André Sampaio Mexias

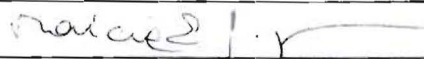
Examinador: Profa. Dra. Márcia Elisa Boscato Gomes

Data: 13/05/2013

Conceito: B

PARECER:

O estudo aborda um tema interessante e representa uma boa contribuição ao assunto. As metodologias utilizadas foram adequadas e muitos dados foram obtidos. As hipóteses levantadas bem como o embasamento teórico foram pouco desenvolvidos. Os resultados poderiam ser mais profundamente discutidos, mas são condizentes com uma dissertação de mestrado.

Assinatura: 

Data:

Ciente do Orientador:

Ciente do Aluno:

Assinatura:

Victor L. Laguardia

Data:

Ciente do Orientador:

[Signature]

Ciente do Aluno: